

Do We Need All the Synthetic Data? Towards Targeted Synthetic Image Augmentation via Diffusion Models

Dang Nguyen*

Department of Computer Science
University of California, Los Angeles
dangnth@cs.ucla.edu

Jiping Li*

Department of Mathematics
University of California, Los Angeles
jipingli0324@g.ucla.edu

Jinghao Zheng*

Department of Automation
Shanghai Jiao Tong University
zjh20030406@sjtu.edu.cn

Baharan Mirzasoleiman

Department of Computer Science
University of California, Los Angeles
baharan@cs.ucla.edu

Abstract

Synthetically augmenting training datasets with diffusion models has been an effective strategy for improving generalization of image classifiers. However, existing techniques struggle to ensure the diversity of generation and increase the size of the data by up to 10-30x to improve the in-distribution performance. In this work, we show that synthetically augmenting part of the data that is not learned early in training outperforms augmenting the entire dataset. By analyzing a two-layer CNN, we prove that this strategy improves generalization by promoting homogeneity in feature learning speed without amplifying noise. Our extensive experiments show that by augmenting only 30%-40% of the data, our method boosts the performance by up to 2.8% in a variety of scenarios, including training ResNet, ViT and DenseNet on CIFAR-10, CIFAR-100, and TinyImageNet, with a range of optimizers including SGD and SAM. Notably, our method applied with SGD outperforms the SOTA optimizer, SAM, on CIFAR-100 and TinyImageNet. It can also easily stack with existing weak and strong augmentation strategies to further boost the performance.

1 Introduction

Data augmentation has been essential to obtaining state-of-the-art in image classification tasks. In particular, adding synthetic images generated by diffusion models [31, 34, 35] improves the accuracy [4] and effective robustness [5] of image classification, beyond what is achieved by weak (random crop, flip, color jitter, etc) and strong data augmentation strategies (PixMix, DeepAugment, etc) [20, 21] or data augmentation using traditional generative models. [7, 18]. Existing works, however, generate synthetic images by conditioning the diffusion model on class labels [4, 5], or noisy versions of entire training data [46]. Unlike weak and strong augmentation techniques, data augmentation techniques based on diffusion models often struggle to ensure diversity and increase the size of the training data by up to 10x [4] to 30x [16] to yield satisfactory performance improvement. This raises a key question:

Does synthetically augmenting the full data yields optimal performance? Can we identify a part of the data that outperforms full data, when synthetically augmented?

At first, this seems implausible as adding synthetic images corresponding to only a part of the training data introduces a shift between training and test data distributions and harms the in-distribution

*Equal contribution.

performance. However, the recent theoretical study of Nguyen et al. [30] revealed a surprising phenomenon: when training with gradient methods, amplifying features that are not learned early in training improves the performance on the *original* data distribution. This is shown by comparing the training dynamics of Sharpness-Aware-Minimization (SAM) with Gradient Descent (GD). SAM is an state-of-the-art optimizer that finds flatter local minima by simultaneously minimizing the value and sharpness of the loss [15]. Empirically, [30] amplified slow-learnable features via a one-shot upsampling of examples that are not learned early in training. Theoretically, one can amplify the slow-learnable features even more to get further performance improvement. However, upsampling such examples more than once resulted in performance degradation, which contradicts the theory.

In our work, we theoretically and empirically address this contradiction. First, by analyzing a two-layer convolutional neural network (CNN), we show that SAM suppresses learning noise from the data. Our results are aligned with that of [10] identifying SAM’s ability in learning less noise as a key factor contributing to its superior generalization performance. Then, we prove that generating faithful synthetic images for the slow-learnable part of the data effectively amplifies their features without amplifying noise. In contrast, upsampling the slow-learnable part of the data amplifies their unique noise, which in turn harms the generalization performance. To generate faithful images, we use real images to guide the diffusion process. This enables synthetically augmenting the slow-learnable part of the data by up to 5x to get further performance improvement. We also prove the faster convergence of synthetic data generation over upsampling, when training with stochastic gradient methods.

We conduct extensive experiments for training ResNet, ViT, and DenseNet on CIFAR10, CIFAR100 [27] and TinyImageNet [28]. We show that our synthetic data augmentation outperforms upsampling or synthetically augmenting the full dataset, and improves SGD and SAM by up to 2.8% by augmenting only 30%-40% of the data. Notably, our method applied with SGD outperforms SAM on CIFAR-100 and TinyImageNet and yields state-of-the-art performance. It can also easily stack with existing weak and strong augmentation strategies to further boost the performance.

2 Related Works

Generative Models for Augmentation. Generative models for data augmentation have become an active area of research with techniques such as GANs [3, 39, 45]. As diffusion models have emerged as a class of powerful generative models, many studies also use synthetic data from diffusion models for data augmentation. For example, Azizi et al. [4] applied diffusion models to ImageNet classification, while further studies [19, 38] explored their application in zero- or few-shot settings. Data augmentation techniques based on diffusion models often struggle to ensure diversity. Thus, recent work [14, 16, 23, 46] has focused on diversifying synthetic images to further enhance performance. Despite the promise, this line of research faces critical challenges. Most notably, these methods are often very complex, as they need to design mechanism to condition the creation of diverse prompts and optimization of conditional embeddings. This hinders their practical applications. Besides, they require to augment the dataset by up to 10x to 20x to demonstrate notable performance improvements. Generating such large volumes of data requires significant computational resources and time.

In our work, we theoretically and empirically study if this large volume of synthetic data is necessary for improving in-distribution performance. Interestingly, we show that synthetically augmenting 30%-40% of examples that are not learned early in training outperforms full data augmentation. Our method is simple and requires much lower computational resources than existing pipelines.

Sharpness-aware-minimization (SAM). SAM is an optimization technique that obtains state-of-the-art performance on a variety of tasks, by simultaneously minimizing the loss and its sharpness [15, 44]. To do so, SAM minimizes the worst-case loss within a neighborhood around the current parameters. In doing so, it doubles the training time. SAM has also been shown to be beneficial in settings such as label noise [15, 44], out-of-distribution [37], and domain generalization [9, 40]. The superior generalization performance of SAM has been contributed to smaller Hessian spectra [6, 15, 25, 41], sparser solution [2], and benign overfitting in presence of weaker signal [10]. Most recently, SAM is shown to learn features at a more uniform speed [30]. In our work, we reveal another key property of SAM contributing to its superior performance: SAM effectively suppresses learning noise from the data. Our results suggest synthetic data generation for slower-learnable part of the data as an effective data augmentation approach for improving the generalization performance.

3 Preliminary

In this section, we introduce our theoretical framework for analyzing synthetic data augmentation with diffusion models. We base our analysis on a simplified data model that reflects the essential structure of image data, where only a small number of features are relevant to the target label. Using this model, we study the training dynamics of a two-layer convolutional neural network. We also discuss how amplifying the slow-learnable features makes training dynamics more similar to SAM.

3.1 Theoretical Setup

Data Distribution. We adopt a similar data distribution used in recent works on feature learning [1, 8, 10, 11, 13, 24, 26] to model data containing two features $\mathbf{v}_d, \mathbf{v}_e$ and noise patches. Formally,

Definition 3.1 (Data distribution). A data point has the form $(\mathbf{x}, y) \sim \mathcal{D}(\beta_e, \beta_d, \alpha) \in (\mathbb{R}^d)^P \times \{\pm 1\}$, where $y \sim \text{Radamacher}(0.5)$, $0 \leq \beta_d < \beta_e \in \mathbb{R}$, and $\mathbf{x} = (\mathbf{x}^{(1)}, \mathbf{x}^{(2)}, \dots, \mathbf{x}^{(P)})$ contains P patches such that for some $\alpha > 0$,

- Exactly one patch is given by the *fast-learnable* feature $\beta_e \cdot y \cdot \mathbf{v}_e$ for some unit vector \mathbf{v}_e with probability α . Otherwise, the patch is given by the *slow-learnable* feature $\beta_d \cdot y \cdot \mathbf{v}_d$ for some unit vector $\mathbf{v}_e \cdot \mathbf{v}_d = 0$.
- The other $P - 1$ patches are i.i.d. Gaussian noise $\boldsymbol{\xi}$ from $\mathcal{N}(0, (\sigma_p^2/d)\mathbf{I}_d)$ for some constant σ_p .

Here probability α controls the frequency of feature \mathbf{v}_e in the data distribution. The distribution parameters β_e, β_d characterize the feature strength in the data. $\beta_e > \beta_d$ ensures that the fast-learnable feature is represented better in the population and thus learned faster. The faster speed of learning captures various notions of simplicity, such as simpler shape, larger magnitude, and less variation. Note that image data in practice are high-dimensional and the noises become dispersed. For simplicity, we assume $P = 2$, that the noise patch is orthogonal from the two features, and that summations involving noise cross-terms $\langle \boldsymbol{\xi}_i, \boldsymbol{\xi}_j \rangle$ become negligible.

Two-layer CNN Model. We use a dataset $D = \{(\mathbf{x}_i, y_i)\}_{i=1}^N$ from distribution 3.1 to train a two-layer nonlinear CNN with activation functions $\sigma(z) = z^3$.

Definition 3.2 (Two-layer CNN). For one data point (\mathbf{x}, y) , the two-layer Convolutional Neural Network (CNN) with weights $\mathbf{W} = [\mathbf{w}_1, \mathbf{w}_2, \dots, \mathbf{w}_J] \in \mathbb{R}^{d \times J}$, where \mathbf{w}_j is weight of the j -th neuron (filter), has the form:

$$f(\mathbf{x}; \mathbf{W}) = \sum_{j=1}^J \sum_{p=1}^P \langle \mathbf{w}_j, \mathbf{x}^{(p)} \rangle^3 = \sum_{j=1}^J \left(\langle \mathbf{w}_j, \boldsymbol{\xi} \rangle^3 + y \begin{cases} \beta_d^3 \langle \mathbf{w}_j, \mathbf{v}_d \rangle^3 & \text{if } \mathbf{v}_d \\ \beta_e^3 \langle \mathbf{w}_j, \mathbf{v}_e \rangle^3 & \text{if } \mathbf{v}_e \end{cases} \right) \quad \text{for our } P = 2.$$

Empirical Risk Minimization. We consider minimizing the following empirical loss:

$$\mathcal{L}(\mathbf{W}) = \frac{1}{N} \sum_{i=1}^N \underbrace{\log(1 + \exp(-y_i f(\mathbf{x}_i; \mathbf{W})))}_{l(y_i f(\mathbf{x}_i; \mathbf{W})), \text{ the logistic loss}}, \quad (1)$$

via (1) sharpness-aware minimization (SAM) [15] and (2) gradient descent (GD), whose filter-wise update rules, with some learning rate $\eta > 0$, are respectively given by:

$$\text{SAM} : \mathbf{w}_j^{(t+1)} = \mathbf{w}_j^{(t)} - \eta \nabla_{\mathbf{w}_j^{(t)}} \mathcal{L}(\mathbf{W}^{(t)} + \rho^{(t)} \nabla \mathcal{L}(\mathbf{W}^{(t)})), \text{ where } \rho^{(t)} = \rho / \|\nabla \mathcal{L}(\mathbf{W}^{(t)})\|_F, \rho > 0,$$

$$\text{GD} : \mathbf{w}_j^{(t+1)} = \mathbf{w}_j^{(t)} - \eta \frac{1}{N} \sum_{i=1}^N \nabla_{i, \mathbf{w}_j^{(t)}} \mathcal{L}(\mathbf{W}^{(t)}) = \mathbf{w}_j^{(t)} - \eta \nabla_{\mathbf{w}_j^{(t)}} \mathcal{L}(\mathbf{W}^{(t)}).$$

Here $\nabla_{\mathbf{w}_j^{(t)}} \mathcal{L}(\mathbf{W}^{(t)})$ denotes the full gradient w.r.t. filter \mathbf{w}_j at iteration t , $\nabla_{i, \mathbf{w}_j^{(t)}} \mathcal{L}(\mathbf{W}^{(t)})$ denotes the per-example gradient for $i \in [N]$, and $\nabla \mathcal{L}(\mathbf{W}^{(t)})$ denotes the full gradient matrix.

High-level idea of SAM. By perturbing the weights with gradient ascent ($\boldsymbol{\epsilon}^{(t)} = \rho^{(t)} \nabla \mathcal{L}(\mathbf{W}^{(t)})$), SAM looks ahead in the *worst* weight direction and forces the training algorithm to escape an unstable (sharp) local minimum. In practice, this has led to more generalizable solutions, while keeping track of two different gradients doubles training time and memory.

3.2 SAM Learns Features More Homogeneously

With the above setting, the alignment of $\mathbf{v}_d, \mathbf{v}_e$ with weights, i.e., $\langle \mathbf{w}^{(t)}, \mathbf{v}_d \rangle$ and $\langle \mathbf{w}^{(t)}, \mathbf{v}_e \rangle$, indicate how much they are learned by the CNN at iteration t . Nguyen et al. [30] showed that SAM’s (normalized) gradient for the *slow-learnable* feature is larger than GD by a factor of

$$k = \left(\frac{1 - \rho^{(t)} \beta_d^3 \langle \mathbf{w}, \mathbf{v}_d \rangle}{1 - \rho^{(t)} \beta_e^3 \langle \mathbf{w}, \mathbf{v}_e \rangle} \right)^{2/3}. \quad (2)$$

That is, SAM amplifies the slow-learnable feature and learns it faster than GD. In doing so, it learns features at a more homogeneous speed.

USEFUL (UpSample Early For Uniform Learning). Motivated by the theory, [30] proposed USEFUL which partitions examples to two clusters after a few training epochs and upsamples the cluster with the higher average loss once ($k = 2$) and restart training on the new data distribution.

While Eq. 2 suggests that the empirical choice of k should depend on the relative strength and difficulty of the features, empirically USEFUL with $k > 2$ resulted in performance degradation, which contradicts the theory. Next, we study this discrepancy between theory and empirical results and show how synthetic data augmentation can effectively bridge the gap.

4 Learning Features More Homogeneously without Overfitting Noise

In this section, we prove that SAM suppresses learning noise from the data. Then, we show that upsampling a part of the data by a factor of k encourages the model to overfit their unique noises, to an extent that scales with k . In contrast, synthetic data augmentation does not suffer from this issue and can effectively amplify features without overfitting noise. Finally, we verify that synthetic data augmentation has superior convergence properties over upsampling.

4.1 SAM Suppresses Learning Noise from the Data

First, we theoretically analyze how SAM suppresses learning noise in the above setting. Intuitively, as SAM pushes the learning dynamics away from sharp landscapes, it simultaneously helps the model avoid areas where certain noises concentrate. This becomes a natural defense against noise overfitting in high-curvature areas. On the other hand, gradient descent is unaware of local smoothness, so it finds solutions that may sit in a flat, noise-resilient basin.

Next, we prove that starting with the same weights $\mathbf{W}^{(t)}$, a SAM step suppresses the model’s alignment with noise directions more effectively than an equivalent gradient step, which performs the regular update. For notations, let Φ denote the sets of noises for dataset D . Let $\mathbf{w}_{j,\epsilon}$ denote the perturbed weights of filter j for SAM. We then define $\mathcal{I}_{j,\epsilon,+}^{(t)} = \{\phi_i \in \Phi : i \in [N], \text{sgn}\langle \mathbf{w}_{j,\epsilon}^{(t)}, \phi_i \rangle = \text{sgn}(y_i)\}$ and $\mathcal{I}_{j,\epsilon,-}^{(t)} = \{\phi_i \in \Phi : i \in [N], \text{sgn}\langle \mathbf{w}_{j,\epsilon}^{(t)}, \phi_i \rangle \neq \text{sgn}(y_i)\}$ be the sets of noises where the sign of alignment matches or mismatches the sign of the label. We define $\mathcal{I}_{j,+}^{(t)}, \mathcal{I}_{j,-}^{(t)}$ accordingly for each GD weight $\mathbf{w}_j^{(t)}$. We measure filter-wise noise learning for a set of noises using the metric $\text{NoiseAlign}(\mathcal{I}, \mathbf{w}_j^{(t)}) = \frac{1}{|\mathcal{I}|} \sum_{\phi \in \mathcal{I}} |\langle \nabla_{\mathbf{w}_j^{(t)}} \mathcal{L}(\mathbf{W}^{(t)}), \phi \rangle|$, which intuitively measures how much noise is learned by the model.

The following theorem quantifies how SAM learns noise to a smaller extent compared to GD. While we analyze the early training phase due to simplicity of analysis, at a high level, our results should still hold during the training.

Theorem 4.1. *With sufficiently large data N and model parameters J , and sufficiently small learning rate η and SAM perturbation parameter ρ , a SAM and a GD update from the same parameters have the following property, early in training:*

1. **Inert Noises:** *Alignment with noises that belong to $\mathcal{I}_{j,-}^{(t)}$ and $\mathcal{I}_{j,\epsilon,-}^{(t)}$ will get closer to 0 after each update, so they will not be learned eventually by GD or SAM.*
2. **Noise Learning:** *The other noises will continue being learned in the sense that $|\langle \mathbf{w}_j, \xi_i \rangle|$ is monotonically increasing. For these noises, SAM slows down noise learning by looking ahead to noise-sensitive (sharp) directions, while GD updates “blindly”. Let $l_i^{(t)} =$*

$\text{sigmoid}(-y_i f(\mathbf{x}_i; \mathbf{W}^{(t)}))$ be the logit term. The following SAM and GD learning dynamics hold for $\xi_i \in \mathcal{I}_{j,\epsilon,+}^{(t)}$ and $\xi_i \in \mathcal{I}_{j,+}^{(t)}$ in terms of noise gradient:

$$\text{SAM: } |\langle \nabla_{\mathbf{w}_{j,\epsilon}} \mathcal{L}(\mathbf{W}^{(t)} + \epsilon^{(t)}), \xi_i \rangle| = \frac{3}{N} l_i^{(t)} \langle \mathbf{w}_j^{(t)}, \xi_i \rangle^2 \left(1 - \frac{3\rho^{(t)}}{N} l_i^{(t)} |\langle \mathbf{w}_j^{(t)}, \xi_i \rangle| \|\xi_i\|^2 \right)^2 \|\xi_i\|^2,$$

$$\text{GD: } |\langle \nabla_{\mathbf{w}_j} \mathcal{L}(\mathbf{W}^{(t)}), \xi_i \rangle| = \frac{3}{N} l_i^{(t)} \langle \mathbf{w}_j^{(t)}, \xi_i \rangle^2 \|\xi_i\|^2.$$

Furthermore, on average, the perturbed SAM gradient aligns strictly less with these noises,

$$\text{NoiseAlign}(\mathcal{I}_{j,\epsilon,+}^{(t)}, \mathbf{w}_{j,\epsilon}^{(t)}) < \text{NoiseAlign}(\mathcal{I}_{j,+}^{(t)}, \mathbf{w}_j^{(t)}).$$

A special case of this theorem is that with the same initializations $\mathbf{W}^{(0)} \sim \mathcal{N}(0, \sigma_0^2)$, nearly half of the noises will not be learned, and SAM in early training prevents overfitting, while GD does not.

All the proof can be found in Appendix A. Our results are aligned with [10] which showed, in a different setting, that SAM's ability to learn less noise contributes to its superior generalization.

Theorem 4.1 implies that to resemble feature learning with SAM and ensure superior convergence, it is crucial to avoid magnifying noise when amplifying the slow-learnable feature. Next, we will show that synthetic data augmentation can achieve the above property, while upsampling fails to do so.

4.2 Synthetic Data Augmentation Amplifies Features But not Noise

Next, we theoretically analyze the effect of synthetically augmenting and upsampling the slow-learnable part of the data by a factor of k on learning dynamics of GD. We show that while both approaches amplify the slow-learnable feature similarly, synthetic data augmentation does not magnify noise and thus has a more similar feature learning behavior to SAM. On the other hand, upsampling encourages the model to overfit the unique noises in the upsampled examples, to an extent that scales with k . In doing so, upsampling with $k > 2$ harms the performance.

Recall that D is the original dataset with $|D| = N$. We assume exactly $(1 - \alpha)N \in \mathbb{Z}$ samples have only \mathbf{v}_d , and let D_U, D_G be the modified datasets via upsampling and generation with factor k and new size $N_{\text{new}} = \alpha N + k(1 - \alpha)N$. For D_U , the replicated noises $\{\xi_i : i = \alpha N + 1, \dots, N\}$ introduce a dependence. Additionally, for D_G , the generative model will have its own noises γ_i (potentially higher than original) for the new data, and we assume the noises are i.i.d., orthogonal to features, and independent from feature noise.

With similar notations, let Φ_G, Φ_U denote the multi-sets² of all the noises for D_G, D_U respectively. We define $\mathcal{I}_{j,+}^{G,(t)} = \{\phi_i \in \Phi_G : i \in [N_{\text{new}}], \text{sgn}(\langle \mathbf{w}_j^{(t)}, \phi_i \rangle) = \text{sgn}(y_i)\}$, $\mathcal{I}_{j,-}^{G,(t)}, \mathcal{I}_{j,+}^{U,(t)}, \mathcal{I}_{j,-}^{U,(t)}$ in a similar fashion for D_G and D_U as before.

Now we are ready to present the following theorem, which suggests that early in training, for feature learning, upsampling and generation contribute similarly, but upsampling accelerates noise learning for noises in $\mathcal{I}_{j,+}^{U,(t)}$, while synthetic generation does not.

Theorem 4.2 (Comparison of feature & noise learning). *Let $\nabla_{\mathbf{w}_j^{(t)}}^U(\mathcal{L}(\mathbf{W}^{(t)}))$ and $\nabla_{\mathbf{w}_j^{(t)}}^G(\mathcal{L}(\mathbf{W}^{(t)}))$ denote the full gradients w.r.t the j -th neuron for upsampling and generation at iteration t respectively. With sufficiently large N, J , sufficiently small learning rate η and noises, starting with the same weights early in training, we expect that for one gradient update,*

1. **Feature Learning & Inert Noises:** Both gradients attempt to contribute equally to feature learning and will not eventually learn certain noises (that are those in $\mathcal{I}_{j,-}^{U,(t)}, \mathcal{I}_{j,-}^{G,(t)}$).
2. **Noise Learning:** Upsampling, compared with generation, amplifies learning of noise on the repeated subset by a factor of k . In particular, for generation, $\phi_i \in \mathcal{I}_{j,\epsilon,+}^{G,(t)}$, where ϕ_i could be ξ_i or the generation noise γ_i ,

$$|\langle \nabla_{\mathbf{w}_j}^G \mathcal{L}(\mathbf{W}^{(t)}), \phi_i \rangle| = \frac{3}{N_{\text{new}}} l_i^{(t)} \langle \mathbf{w}_j^{(t)}, \phi_i \rangle^2 \|\phi_i\|^2.$$

²Due to identical noises in D_U . The following $\mathcal{I}_{j,+}^{U,(t)}$ and $\mathcal{I}_{j,-}^{U,(t)}$ are also multi-sets to keep their sizes consistent with the generation counterparts, meaning that we count all the replicated noises.

However, for upsampling, $\xi_i \in \mathcal{I}_{j,+}^{U,(t)}$,

$$|\langle \nabla_{\mathbf{w}_j}^U \mathcal{L}(\mathbf{W}^{(t)}), \xi_i \rangle| = \begin{cases} \frac{3}{N_{new}} l_i^{(t)} \langle \mathbf{w}_j^{(t)}, \xi_i \rangle^2 \|\xi_i\|^2, & i = 1, \dots, \alpha N \\ \frac{3k}{N_{new}} l_i^{(t)} \langle \mathbf{w}_j^{(t)}, \xi_i \rangle^2 \|\xi_i\|^2, & i = \alpha N + 1, \dots, N \end{cases}.$$

A special case of this theorem is that with the same initializations $\mathbf{W}^{(0)} \sim \mathcal{N}(0, \sigma_0^2)$, informally, we expect $\mathbf{NoiseAlign}(\mathcal{I}_{j,+}^{G,(t)}, \mathbf{w}_j^{(t)}) < \mathbf{NoiseAlign}(\mathcal{I}_{j,+}^{U,(t)}, \mathbf{w}_j^{(t)})$ for all the early iterations $0 \leq t \leq T$, if the generation noise is sufficiently small in the sense that in expectation,

$$\langle \mathbf{w}_j^{(0)}, \gamma \rangle^2 \|\gamma\|^2 < (k+1) \langle \mathbf{w}_j^{(0)}, \xi \rangle^2 \|\xi\|^2 \quad \text{for some data noise } \xi \text{ and generation noise } \gamma.$$

Theorem 4.2 captures one important observation in practice that not all the noises are created equal. Additionally, we note that for generation, the update rules learn each noise in a similar fashion, but for upsampling, we still only have N unique noises, and the training dynamics deviates more from SAM for the extra learning on the upsampled ones. Consequently, choosing $k > 2$ increasingly pushes the model toward overfitting particular noises—explaining the empirically observed performance drop of upsampling at larger k for USEFUL.

Remark. Intuitively, for a diffusion model, as long as the noises in the synthetic data $\|\gamma_i\|^2$ are not too large, noise learning under generation is more diffused due to its independence and operates more similarly to SAM, whereas upsampling amplifies learning on the duplicated noise, potentially elevating it to a new feature and increasing the **NoiseAlign** metric.

4.3 Superior Convergence of Synthetic Data Augmentation over Upsampling

Next, we compare the convergence of mini-batch Stochastic Gradient Descent (SGD)—which is used in practice—on synthetically augmented and upsampled data and confirm the superior convergence of synthetic data augmentation. Consider training the above CNN using SGD with batch size B :

$$\mathbf{w}_j^{(t+1)} = \mathbf{w}_j^{(t)} - \eta \frac{1}{B} \sum_{i=1}^B \nabla_{i, \mathbf{w}_j^{(t)}} \mathcal{L}(\mathbf{W}^{(t)}).$$

The convergence rate of mini-batch SGD is inversely proportional to the batch size [17]. The following theorem shows that upsampling inflates the variance of mini-batch gradients and consequently slows down convergence. Note that it does not directly compare the relative magnitudes of the variances, since $\sigma_G(k)$, $\sigma_U(k)$ depend on datasets. Instead, it quantifies the sources of extra variance:

Theorem 4.3 (Variance of mini-batch gradients). *Suppose we train the model using mini-batch SGD with proper batch size B . Let $\mathbb{E}_{i \in D_G} [\|\mathbf{g}_i - \bar{\mathbf{g}}_G\|^2] \leq \sigma_G^2(k)$, $\mathbb{E}_{i \in D_U} [\|\mathbf{g}_i - \bar{\mathbf{g}}_U\|^2] \leq \sigma_U^2(k)$ be the variances of the per-example gradients for generation and upsampling (where \mathbf{g}_i is the gradient of the i -th data and $\bar{\mathbf{g}}$ is the full gradient). Let $\hat{\mathbf{g}}_U$ and $\hat{\mathbf{g}}_G$ be the mini-batch gradients. We have:*

$$\mathbb{E}_{D_G} [\|\hat{\mathbf{g}}_G - \bar{\mathbf{g}}_G\|^2] \leq \frac{\sigma_G^2(k)}{B},$$

$$\mathbb{E}_{D_U} [\|\hat{\mathbf{g}}_U - \bar{\mathbf{g}}_U\|^2] \leq I, \quad \text{where } I \geq \frac{\sigma_U^2(k)}{B} \left(1 + \frac{k(k-1)(1-\alpha) B}{(\alpha + k(1-\alpha))^2 N} \right).$$

From Theorem 4.3, we see that all the variance for generation comes from the per-example variance, potentially getting larger when synthetic images diversify the dataset. However, upsampling induces one extra term that results from repeated noises and unnecessarily inflates the variance due to dependence within the dataset. This is empirically justified in our ablation studies in Section 5.4.

Corollary 4.4. *As long as the generation noise is small enough, i.e., $\sigma_G^2(k) < \sigma_U^2(k)$, convergence of mini-batch SGD on synthetically augmented data is faster than upsampled data.*

4.4 Generating Faithful Synthetic Images via Diffusion Models

Finally, we discuss generating faithful images for the slow-learnable part of the data. From Theorem 4.2 we know that while the noise in the synthetic data can be larger than that of the original data, it should be small enough to yield a similar feature learning behavior to SAM.

Synthetic image generation with diffusion models [22, 32, 36, 42] involves a forward process to iteratively add noise to the images, followed by a reverse process to learn to denoise the images. Specifically, the forward process progressively adds noise to the data x_0 over T steps, with each step modeled as a Gaussian transition: $q(\mathbf{x}_t|\mathbf{x}_{t-1}) = \mathcal{N}(\mathbf{x}_t; \sqrt{1 - \beta_t}\mathbf{x}_{t-1}, \beta_t\mathbf{I})$, where β_t controls the noise added at each step. The reverse process inverts the forward process, learns to denoise the data, with the goal of recovering the original data x_0 from a noisy sample x_T : $p_\theta(\mathbf{x}_{t-1}|\mathbf{x}_t) = \mathcal{N}(\mathbf{x}_{t-1}; \mu_\theta(\mathbf{x}_t, t), \Sigma_\theta(\mathbf{x}_t, t))$, where mean μ_θ is conditioned on the sample at the previous time step and variance Σ_θ follows a fixed schedule.

To ensure generating images that are faithful to real data, we use the real images as guidance to generate synthetic images. Specifically, while using the class name (e.g., “a photo of a dog”) as the text prompt, we also incorporated the original real samples as guidance. More formally, instead of sampling a pure noisy image $x_T \sim \mathcal{N}(0, I)$ as the initialization of the reverse path, we add noise to a reference (real) image x_0^{ref} such that the noise level corresponds to a certain time-step t_* . Then we begin denoising from time-step t_* , using an open-source text-to-image model, e.g. GLIDE [31], to iteratively predict a less noisy image x_{t-1} ($t = T, T-1, \dots, 1$) using the given text prompt l and the noisy latent image x_t as inputs. This technique enables produce synthetic images that are similar, yet distinct, from the original examples, and has been successfully used for synthetic image generation for few-shot learning [19].

The pseudocode of our method is illustrated in Alg. 1 in Appendix E. Our algorithm is similar to USEFUL except that in Step 3, we replace the real images by synthetic images generated as above.

5 Experiment

In this section, we evaluate the effectiveness of our synthetic augmentation strategy on various datasets and model architectures. We also conduct an ablation study on different parts of our method.

5.1 Settings

Base training datasets. We use common benchmark datasets for image classification including CIFAR10, CIFAR100 [27], and Tiny-ImageNet [28] for image classification.

Augmented training datasets. We train different models on: (1) **Original**: The original training datasets without any modifications. (2) **USEFUL**: Augmented dataset with upsampled real images that are not learned in early training. (3) **Our Method**: Replace the upsampled samples in USEFUL with their corresponding synthetic images. For $k > 2$, we use generated images at different diffusion denoising steps, instead of generating from scratch.

Training details. We train ResNet18 on all datasets following the setting of [2]. The models are trained for 200 epochs with a batch size of 128. We use SGD with the momentum parameter 0.9 and set weight decay to 0.0005. We also fix $\rho = 0.1$ for SAM in all experiments. We use a linear learning rate schedule starting at 0.1 and decay by a factor of 10 once at epoch 100 and again at epoch 150. For each setup, we perform training using two different optimization methods: SGD and SAM.

Hyperparameters. For USEFUL [30], we adopt their default hyper-parameters for separating epochs and set the upsampling factor k to 2 as it yields the best performance. For our method, the upsampling factor k is set to 5 for CIFAR10 and CIFAR100 while that of TinyImageNet is set to 4. For generating synthetic images using GLIDE, we use guidance scale of 3 and run denoising for 100 steps, saving generated images every 10 steps.

More details about the experimental settings can be found in Appendix F.1.

5.2 Our Method is Effective across Datasets and Architectures

Different datasets. Figure 1 clearly shows that our method significantly reduces the test classification error compared to both the **Original** and **USEFUL** methods across all datasets, namely CIFAR10, CIFAR100, and Tiny-ImageNet. For Tiny ImageNet, our method yields an improvement of more than 2% regardless of the optimizer choice. The superior performance of our method compared to USEFUL is well aligned with our theoretical results in Section 4.3. Notably, SGD with our method outperforms SAM on CIFAR100 and TinyImageNet. This clearly confirms the effectiveness of our approach.

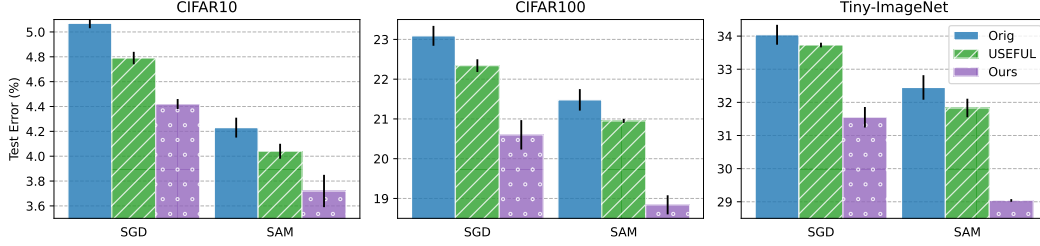


Figure 1: Test classification error of ResNet18 on CIFAR10, CIFAR100 and TinyImageNet. For USEFUL, the upsampling factor k is always set to 2 while for Ours, k is set to 5, 5, and 4 for CIFAR10, CIFAR100, and Tiny-ImageNet, respectively. Our method improves both SGD and SAM. Notably, it enables SGD to outperform SAM on CIFAR100 and TinyImageNet.

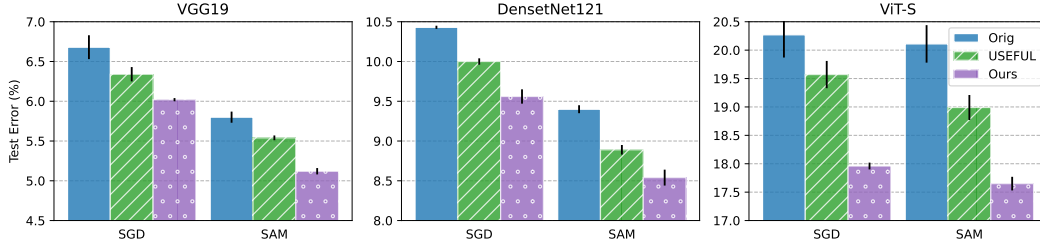


Figure 2: Test classification error of VGG19, DenseNet121, and ViT-S on CIFAR10. For USEFUL, the upsampling factor k is set to 2 while for Ours, k is set to 5.

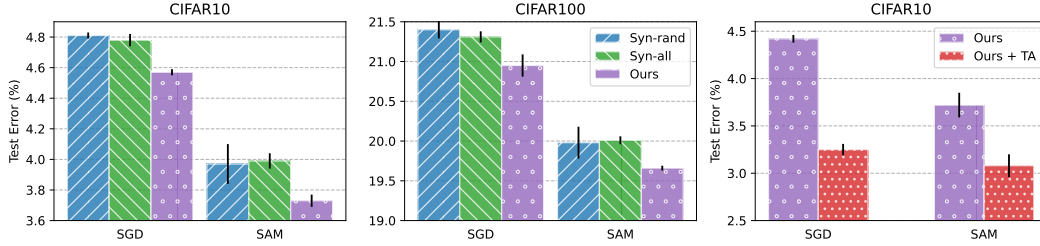


Figure 3: (left & middle) Comparison between different synthetic image augmentation strategies when training ResNet18 on CIFAR10 and CIFAR100. The upsampling factor k is set to 2 for Syn-rand and Ours, resulting in only 30% and 40% additional examples compared to 100% of Syn-all. (right) Our method with $k = 5$ can be stacked with TrivialAugment (TA) to further boosts the performance when training ResNet18 on CIFAR10, achieving (to our knowledge) SOTA test classification error.

Different model architectures. To further evaluate the generalization of our approach, we conduct experiments on multiple model architectures using **CIFAR10** as the base dataset. Specifically, we apply our method to CNNs (VGG19, DenseNet121) and Transformers (ViT-S). Figure 2 presents the test classification error for different architectures. The results demonstrate that our method achieves consistently lower classification error than both the **Original** and **USEFUL** methods across all architectures, under both SGD and SAM optimization settings. These findings further confirm the robustness and effectiveness of our approach across different network structures.

5.3 Do We Need All the Synthetic Data?

To answer the question “Do We Need All the Synthetic Data?”, we mix all the corresponding generated images with the training data at a 1:1 ratio, doubling the training set size, denoted as **Syn-all**. In this case, we set $k = 2$ in our method, resulting in increase of approximately 30% and 40% of the total training data in CIFAR10 and CIFAR100, respectively. This means that the computational cost of generating these samples is much lower than that of **Syn-all**, which requires 100% of the training data to be augmented with generated images. Consequently, the generation time for our method is

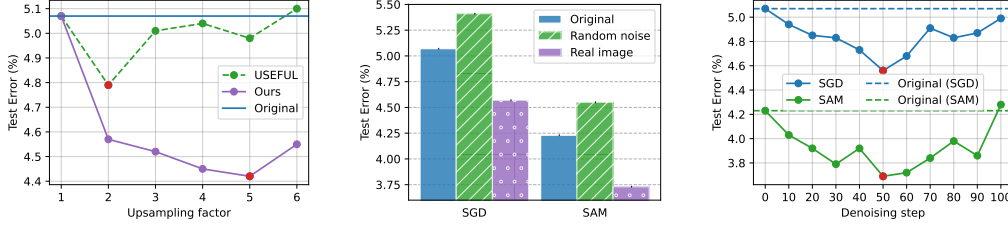


Figure 4: (left) The effect of the upsampling factor k on the performance of training ResNet18 with SGD on the augmented CIFAR10 dataset produced by our method and USEFUL. Red points indicate the optimal choice of k for each method. (middle) Comparison between synthetic CIFAR10 images generated from random noises and real images when training ResNet18 on the augmented set with $k = 2$. For reference, we include the performance of the original training set. (right) The effect of the number of denoising steps on the performance of training ResNet18 on the augmented CIFAR10 dataset produced by our method with $k = 2$.

reduced to 0.3x and 0.4x that of **Syn-all**, making it more efficient. In addition, we consider a baseline (**Syn-rand**) where random images are augmented with their corresponding synthetic ones. In terms of the test classification error, our method outperforms both **Syn-rand** (same cost) and **Syn-all** (higher cost) as shown in Figure 3. This highlights the effectiveness of our targeted augmentation compared to random augmentation or simply augmenting all the images.

5.4 Ablation studies

Our method can be stacked with strong augmentation methods. Figure 3 right shows that our method stacked with TrivialAugment [29] achieves state-of-the-art results when training ResNet18 on CIFAR10. Appendix F.2 shows similar results for CIFAR100 and Tiny-ImageNet.

Effect of the upsampling factor. Figure 4a illustrates the performance of our method and USEFUL on CIFAR10 when varying the upsampling factors. As discussed in Section 3.2, USEFUL achieves the best performance at $k = 2$ due to overfitting noise at larger k . On the other hand, using synthetic images, our method benefits from larger values of k , yielding the best performance at $k = 5$ for CIFAR10 and CIFAR100, and $k = 4$ for Tiny-ImageNet. Detailed results for CIFAR100 and Tiny-ImageNet can be found in Table 2 in Appendix F.2. This corroborates our theoretical findings in Section 4.2.

Choices of initialization for denoising. To validate the necessity of our faithful synthetic image generation pipeline, we run a baseline where synthetic images are generated using the standard diffusion pipeline, i.e., denoised from random noises instead of the real images. Figure 4b illustrates that faithful synthetic images are necessary for targeted synthetic image augmentation. When using random noises to generate synthetic images, the performance of ResNet18 on the augmented training datasets is even worse than that on the original set. This is because the generated images are not close enough to real images, resulting in a large noise which in turn harms the model performance as discussed in Theorem 4.2.

Effect of the number of denoising steps. Figure 4c demonstrates the effect of the number of denoising steps on the performance of our method. Using fewer steps generates images that are too close to real images, amplifying the noise in the real images. On the other hand, using too many steps results in too much noise, which also harms the performance. Overall, using 50 steps yields the best results for both SGD and SAM.

Convergence. Figure 5 in Appendix F.2 shows the mini-batch gradient variance when training ResNet18 with SGD on the augmented CIFAR10 dataset found by USEFUL and Ours. It can be seen that training on our augmented datasets results in lower gradient variance at every upsampling factor k . This confirms our theoretical results in Theorem 4.3 and Corollary 4.4.

6 Conclusion

In this work, we show that synthetically augmenting part of the data that is not learned early in training outperforms augmenting the entire dataset. By analyzing a two-layer CNN, we prove that this method allows features to be learned at a more uniform speed without amplifying noise. We

conducted extensive experiments showing that our augmentation strategy boosts the performance when training ResNet, ViT and DenseNet on CIFAR-10, CIFAR-100, and TinyImageNet, with a range of optimizers including SGD and SAM, by up to 2.8%. Notably, our method applied with SGD outperforms SAM on CIFAR-100 and TinyImageNet and easily stacks with existing weak and strong data augmentation strategies to obtain state-of-the-art performance.

References

- [1] Zeyuan Allen-Zhu and Yuanzhi Li. Towards understanding ensemble, knowledge distillation and self-distillation in deep learning. *arXiv preprint arXiv:2012.09816*, 2020.
- [2] Maksym Andriushchenko and Nicolas Flammarion. Towards understanding sharpness-aware minimization. In *International Conference on Machine Learning*, pages 639–668. PMLR, 2022.
- [3] Antreas Antoniou, Amos Storkey, and Harrison Edwards. Data augmentation generative adversarial networks, 2018. URL <https://arxiv.org/abs/1711.04340>.
- [4] Shekoofeh Azizi, Simon Kornblith, Chitwan Saharia, Mohammad Norouzi, and David J. Fleet. Synthetic Data from Diffusion Models Improves ImageNet Classification, April 2023. URL <http://arxiv.org/abs/2304.08466>. arXiv:2304.08466 [cs].
- [5] Hritik Bansal and Aditya Grover. Leaving reality to imagination: Robust classification via generated datasets. *arXiv preprint arXiv:2302.02503*, 2023.
- [6] Peter L Bartlett, Philip M Long, and Olivier Bousquet. The dynamics of sharpness-aware minimization: Bouncing across ravines and drifting towards wide minima. *Journal of Machine Learning Research*, 24(316):1–36, 2023.
- [7] Andrew Brock, Jeff Donahue, and Karen Simonyan. Large scale gan training for high fidelity natural image synthesis. *arXiv preprint arXiv:1809.11096*, 2018.
- [8] Yuan Cao, Zixiang Chen, Misha Belkin, and Quanquan Gu. Benign overfitting in two-layer convolutional neural networks. *Advances in neural information processing systems*, 35:25237–25250, 2022.
- [9] Junbum Cha, Sanghyuk Chun, Kyungjae Lee, Han-Cheol Cho, Seunghyun Park, Yunsung Lee, and Sungrae Park. Swad: Domain generalization by seeking flat minima. In M. Ranzato, A. Beygelzimer, Y. Dauphin, P.S. Liang, and J. Wortman Vaughan, editors, *Advances in Neural Information Processing Systems*, volume 34, pages 22405–22418. Curran Associates, Inc., 2021. URL https://proceedings.neurips.cc/paper_files/paper/2021/file/bcb41ccdc4363c6848a1d760f26c28a0-Paper.pdf.
- [10] Zixiang Chen, Yihe Deng, Yue Wu, Quanquan Gu, and Yuanzhi Li. Towards understanding the mixture-of-experts layer in deep learning. *Advances in neural information processing systems*, 35:23049–23062, 2022.
- [11] Zixiang Chen, Junkai Zhang, Yiwen Kou, Xiangning Chen, Cho-Jui Hsieh, and Quanquan Gu. Why does sharpness-aware minimization generalize better than sgd? *arXiv preprint arXiv:2310.07269*, 2023.
- [12] Jia Deng, Wei Dong, Richard Socher, Li-Jia Li, Kai Li, and Li Fei-Fei. Imagenet: A large-scale hierarchical image database. In *2009 IEEE conference on computer vision and pattern recognition*, pages 248–255. Ieee, 2009.
- [13] Yihe Deng, Yu Yang, Baharan Mirzasoleiman, and Quanquan Gu. Robust learning with progressive data expansion against spurious correlation. *arXiv preprint arXiv:2306.04949*, 2023.
- [14] Lisa Dunlap, Alyssa Umino, Han Zhang, Jiezhi Yang, Joseph E. Gonzalez, and Trevor Darrell. Diversify Your Vision Datasets with Automatic Diffusion-Based Augmentation, October 2023. URL <http://arxiv.org/abs/2305.16289>. arXiv:2305.16289 [cs].
- [15] Pierre Foret, Ariel Kleiner, Hossein Mobahi, and Behnam Neyshabur. Sharpness-aware minimization for efficiently improving generalization. *arXiv preprint arXiv:2010.01412*, 2020.

- [16] Yunxiang Fu, Chaoqi Chen, Yu Qiao, and Yizhou Yu. DreamDA: Generative Data Augmentation with Diffusion Models, March 2024. URL <http://arxiv.org/abs/2403.12803>. arXiv:2403.12803 [cs].
- [17] Saeed Ghadimi and Guanghui Lan. Stochastic first-and zeroth-order methods for nonconvex stochastic programming. *SIAM journal on optimization*, 23(4):2341–2368, 2013.
- [18] Ian Goodfellow, Jean Pouget-Abadie, Mehdi Mirza, Bing Xu, David Warde-Farley, Sherjil Ozair, Aaron Courville, and Yoshua Bengio. Generative adversarial networks. *Communications of the ACM*, 63(11):139–144, 2020.
- [19] Ruifei He, Shuyang Sun, Xin Yu, Chuhui Xue, Wenqing Zhang, Philip Torr, Song Bai, and Xiaojuan Qi. Is synthetic data from generative models ready for image recognition?, February 2023. URL <http://arxiv.org/abs/2210.07574>. arXiv:2210.07574 [cs].
- [20] Dan Hendrycks, Steven Basart, Norman Mu, Saurav Kadavath, Frank Wang, Evan Dorundo, Rahul Desai, Tyler Zhu, Samyak Parajuli, Mike Guo, et al. The many faces of robustness: A critical analysis of out-of-distribution generalization. In *Proceedings of the IEEE/CVF International Conference on Computer Vision*, pages 8340–8349, 2021.
- [21] Dan Hendrycks, Andy Zou, Mantas Mazeika, Leonard Tang, Bo Li, Dawn Song, and Jacob Steinhardt. Pixmix: Dreamlike pictures comprehensively improve safety measures. In *Proceedings of the IEEE/CVF Conference on Computer Vision and Pattern Recognition*, pages 16783–16792, 2022.
- [22] Jonathan Ho, Ajay Jain, and Pieter Abbeel. Denoising Diffusion Probabilistic Models. In H. Larochelle, M. Ranzato, R. Hadsell, M. F. Balcan, and H. Lin, editors, *Advances in Neural Information Processing Systems*, volume 33, pages 6840–6851. Curran Associates, Inc., 2020. URL https://proceedings.neurips.cc/paper_files/paper/2020/file/4c5bcfec8584af0d967f1ab10179ca4b-Paper.pdf.
- [23] Khawar Islam, Muhammad Zaigham Zaheer, Arif Mahmood, and Karthik Nandakumar. DiffuseMix: Label-Preserving Data Augmentation with Diffusion Models, April 2024. URL <http://arxiv.org/abs/2405.14881>. arXiv:2405.14881 [cs].
- [24] Samy Jelassi and Yuanzhi Li. Towards understanding how momentum improves generalization in deep learning. In *International Conference on Machine Learning*, pages 9965–10040. PMLR, 2022.
- [25] Simran Kaur, Jeremy Cohen, and Zachary Chase Lipton. On the maximum hessian eigenvalue and generalization. In *Proceedings on*, pages 51–65. PMLR, 2023.
- [26] Yiwen Kou, Zixiang Chen, Yuanzhou Chen, and Quanquan Gu. Benign overfitting in two-layer relu convolutional neural networks. In *International Conference on Machine Learning*, pages 17615–17659. PMLR, 2023.
- [27] Alex Krizhevsky, Geoffrey Hinton, et al. Learning multiple layers of features from tiny images. *Technical Report, University of Toronto*, 2009.
- [28] Yann Le and Xuan Yang. Tiny imagenet visual recognition challenge. *CS 231N*, 7(7):3, 2015.
- [29] Samuel G. Müller and Frank Hutter. Trivialaugment: Tuning-free yet state-of-the-art data augmentation. In *Proceedings of the IEEE/CVF International Conference on Computer Vision (ICCV)*, pages 774–782, October 2021.
- [30] Dang Nguyen, Paymon Haddad, Eric Gan, and Baharan Mirzasoleiman. Changing the training data distribution to reduce simplicity bias improves in-distribution generalization. *Advances in Neural Information Processing Systems*, 37:68854–68896, 2024.
- [31] Alex Nichol, Prafulla Dhariwal, Aditya Ramesh, Pranav Shyam, Pamela Mishkin, Bob McGrew, Ilya Sutskever, and Mark Chen. Glide: Towards photorealistic image generation and editing with text-guided diffusion models. *arXiv preprint arXiv:2112.10741*, 2021.

- [32] Alexander Quinn Nichol and Prafulla Dhariwal. Improved denoising diffusion probabilistic models. In Marina Meila and Tong Zhang, editors, *Proceedings of the 38th International Conference on Machine Learning*, volume 139 of *Proceedings of Machine Learning Research*, pages 8162–8171. PMLR, 18–24 Jul 2021. URL <https://proceedings.mlr.press/v139/nichol21a.html>.
- [33] Adam Paszke, Sam Gross, Francisco Massa, Adam Lerer, James Bradbury, Gregory Chanan, Trevor Killeen, Zeming Lin, Natalia Gimelshein, Luca Antiga, Alban Desmaison, Andreas Kopf, Edward Yang, Zachary DeVito, Martin Raison, Alykhan Tejani, Sasank Chilamkurthy, Benoit Steiner, Lu Fang, Junjie Bai, and Soumith Chintala. PyTorch: An Imperative Style, High-Performance Deep Learning Library. In H. Wallach, H. Larochelle, A. Beygelzimer, F. d’Alché-Buc, E. Fox, and R. Garnett, editors, *Advances in Neural Information Processing Systems*, volume 32. Curran Associates, Inc., 2019. URL https://proceedings.neurips.cc/paper_files/paper/2019/file/bdbca288fee7f92f2bfa9f7012727740-Paper.pdf.
- [34] Robin Rombach, Andreas Blattmann, Dominik Lorenz, Patrick Esser, and Björn Ommer. High-resolution image synthesis with latent diffusion models. In *Proceedings of the IEEE/CVF conference on computer vision and pattern recognition*, pages 10684–10695, 2022.
- [35] Chitwan Saharia, William Chan, Saurabh Saxena, Lala Li, Jay Whang, Emily L Denton, Kamyar Ghasemipour, Raphael Gontijo Lopes, Burcu Karagol Ayan, Tim Salimans, et al. Photorealistic text-to-image diffusion models with deep language understanding. *Advances in Neural Information Processing Systems*, 35:36479–36494, 2022.
- [36] Jascha Sohl-Dickstein, Eric Weiss, Niru Maheswaranathan, and Surya Ganguli. Deep unsupervised learning using nonequilibrium thermodynamics. In Francis Bach and David Blei, editors, *Proceedings of the 32nd International Conference on Machine Learning*, volume 37 of *Proceedings of Machine Learning Research*, pages 2256–2265, Lille, France, 07–09 Jul 2015. PMLR. URL <https://proceedings.mlr.press/v37/sohl-dickstein15.html>.
- [37] Jacob Mitchell Springer, Vaishnavh Nagarajan, and Aditi Raghunathan. Sharpness-aware minimization enhances feature quality via balanced learning. In *The Twelfth International Conference on Learning Representations*, 2024.
- [38] Brandon Trabucco, Kyle Doherty, Max Gurinas, and Ruslan Salakhutdinov. Effective Data Augmentation With Diffusion Models, May 2023. URL <http://arxiv.org/abs/2302.07944>. arXiv:2302.07944 [cs].
- [39] Toan Tran, Trung Pham, Gustavo Carneiro, Lyle Palmer, and Ian Reid. A Bayesian Data Augmentation Approach for Learning Deep Models. In I. Guyon, U. Von Luxburg, S. Bengio, H. Wallach, R. Fergus, S. Vishwanathan, and R. Garnett, editors, *Advances in Neural Information Processing Systems*, volume 30. Curran Associates, Inc., 2017. URL https://proceedings.neurips.cc/paper_files/paper/2017/file/076023edc9187cf1ac1f1163470e479a-Paper.pdf.
- [40] Pengfei Wang, Zhaoxiang Zhang, Zhen Lei, and Lei Zhang. Sharpness-aware gradient matching for domain generalization. In *Proceedings of the IEEE/CVF Conference on Computer Vision and Pattern Recognition (CVPR)*, pages 3769–3778, June 2023.
- [41] Kaiyue Wen, Tengyu Ma, and Zhiyuan Li. How does sharpness-aware minimization minimize sharpness? *arXiv preprint arXiv:2211.05729*, 2022.
- [42] Ling Yang, Zhilong Zhang, Yang Song, Shenda Hong, Runsheng Xu, Yue Zhao, Wentao Zhang, Bin Cui, and Ming-Hsuan Yang. Diffusion models: A comprehensive survey of methods and applications. *ACM Comput. Surv.*, 56(4), November 2023. ISSN 0360-0300. doi: 10.1145/3626235. URL <https://doi.org/10.1145/3626235>.
- [43] Li Yuan, Yunpeng Chen, Tao Wang, Weihao Yu, Yujun Shi, Zi-Hang Jiang, Francis E.H. Tay, Jiashi Feng, and Shuicheng Yan. Tokens-to-token vit: Training vision transformers from scratch on imagenet. In *Proceedings of the IEEE/CVF International Conference on Computer Vision (ICCV)*, pages 558–567, October 2021.

- [44] Yaowei Zheng, Richong Zhang, and Yongyi Mao. Regularizing neural networks via adversarial model perturbation. In *Proceedings of the IEEE/CVF Conference on Computer Vision and Pattern Recognition (CVPR)*, pages 8156–8165, June 2021.
- [45] Zhedong Zheng, Liang Zheng, and Yi Yang. Unlabeled samples generated by gan improve the person re-identification baseline in vitro. In *2017 IEEE International Conference on Computer Vision (ICCV)*, pages 3774–3782, 2017. doi: 10.1109/ICCV.2017.405.
- [46] Yongchao Zhou, Hshmat Sahak, and Jimmy Ba. Training on thin air: Improve image classification with generated data. *arXiv preprint arXiv:2305.15316*, 2023.

NeurIPS Paper Checklist

The checklist is designed to encourage best practices for responsible machine learning research, addressing issues of reproducibility, transparency, research ethics, and societal impact. Do not remove the checklist: **The papers not including the checklist will be desk rejected.** The checklist should follow the references and follow the (optional) supplemental material. The checklist does NOT count towards the page limit.

Please read the checklist guidelines carefully for information on how to answer these questions. For each question in the checklist:

- You should answer [Yes], [No], or [NA].
- [NA] means either that the question is Not Applicable for that particular paper or the relevant information is Not Available.
- Please provide a short (1–2 sentence) justification right after your answer (even for NA).

The checklist answers are an integral part of your paper submission. They are visible to the reviewers, area chairs, senior area chairs, and ethics reviewers. You will be asked to also include it (after eventual revisions) with the final version of your paper, and its final version will be published with the paper.

The reviewers of your paper will be asked to use the checklist as one of the factors in their evaluation. While "[Yes]" is generally preferable to "[No]", it is perfectly acceptable to answer "[No]" provided a proper justification is given (e.g., "error bars are not reported because it would be too computationally expensive" or "we were unable to find the license for the dataset we used"). In general, answering "[No]" or "[NA]" is not grounds for rejection. While the questions are phrased in a binary way, we acknowledge that the true answer is often more nuanced, so please just use your best judgment and write a justification to elaborate. All supporting evidence can appear either in the main paper or the supplemental material, provided in appendix. If you answer [Yes] to a question, in the justification please point to the section(s) where related material for the question can be found.

IMPORTANT, please:

- **Delete this instruction block, but keep the section heading “NeurIPS Paper Checklist”,**
- **Keep the checklist subsection headings, questions/answers and guidelines below.**
- **Do not modify the questions and only use the provided macros for your answers.**

1. Claims

Question: Do the main claims made in the abstract and introduction accurately reflect the paper’s contributions and scope?

Answer: [Yes]

Justification: Our claims match the theoretical and experimental results.

Guidelines:

- The answer NA means that the abstract and introduction do not include the claims made in the paper.
- The abstract and/or introduction should clearly state the claims made, including the contributions made in the paper and important assumptions and limitations. A No or NA answer to this question will not be perceived well by the reviewers.
- The claims made should match theoretical and experimental results, and reflect how much the results can be expected to generalize to other settings.
- It is fine to include aspirational goals as motivation as long as it is clear that these goals are not attained by the paper.

2. Limitations

Question: Does the paper discuss the limitations of the work performed by the authors?

Answer: [Yes]

Justification: We provide full assumptions in both the main text and Appendix.

Guidelines:

- The answer NA means that the paper has no limitation while the answer No means that the paper has limitations, but those are not discussed in the paper.
- The authors are encouraged to create a separate "Limitations" section in their paper.
- The paper should point out any strong assumptions and how robust the results are to violations of these assumptions (e.g., independence assumptions, noiseless settings, model well-specification, asymptotic approximations only holding locally). The authors should reflect on how these assumptions might be violated in practice and what the implications would be.
- The authors should reflect on the scope of the claims made, e.g., if the approach was only tested on a few datasets or with a few runs. In general, empirical results often depend on implicit assumptions, which should be articulated.
- The authors should reflect on the factors that influence the performance of the approach. For example, a facial recognition algorithm may perform poorly when image resolution is low or images are taken in low lighting. Or a speech-to-text system might not be used reliably to provide closed captions for online lectures because it fails to handle technical jargon.
- The authors should discuss the computational efficiency of the proposed algorithms and how they scale with dataset size.
- If applicable, the authors should discuss possible limitations of their approach to address problems of privacy and fairness.
- While the authors might fear that complete honesty about limitations might be used by reviewers as grounds for rejection, a worse outcome might be that reviewers discover limitations that aren't acknowledged in the paper. The authors should use their best judgment and recognize that individual actions in favor of transparency play an important role in developing norms that preserve the integrity of the community. Reviewers will be specifically instructed to not penalize honesty concerning limitations.

3. Theory assumptions and proofs

Question: For each theoretical result, does the paper provide the full set of assumptions and a complete (and correct) proof?

Answer: [\[Yes\]](#)

Justification: We provide full assumptions and proofs in Appendix.

Guidelines:

- The answer NA means that the paper does not include theoretical results.
- All the theorems, formulas, and proofs in the paper should be numbered and cross-referenced.
- All assumptions should be clearly stated or referenced in the statement of any theorems.
- The proofs can either appear in the main paper or the supplemental material, but if they appear in the supplemental material, the authors are encouraged to provide a short proof sketch to provide intuition.
- Inversely, any informal proof provided in the core of the paper should be complemented by formal proofs provided in appendix or supplemental material.
- Theorems and Lemmas that the proof relies upon should be properly referenced.

4. Experimental result reproducibility

Question: Does the paper fully disclose all the information needed to reproduce the main experimental results of the paper to the extent that it affects the main claims and/or conclusions of the paper (regardless of whether the code and data are provided or not)?

Answer: [\[Yes\]](#)

Justification: We provide detailed experimental settings in the Experiment section and in Appendix.

Guidelines:

- The answer NA means that the paper does not include experiments.

- If the paper includes experiments, a No answer to this question will not be perceived well by the reviewers: Making the paper reproducible is important, regardless of whether the code and data are provided or not.
- If the contribution is a dataset and/or model, the authors should describe the steps taken to make their results reproducible or verifiable.
- Depending on the contribution, reproducibility can be accomplished in various ways. For example, if the contribution is a novel architecture, describing the architecture fully might suffice, or if the contribution is a specific model and empirical evaluation, it may be necessary to either make it possible for others to replicate the model with the same dataset, or provide access to the model. In general, releasing code and data is often one good way to accomplish this, but reproducibility can also be provided via detailed instructions for how to replicate the results, access to a hosted model (e.g., in the case of a large language model), releasing of a model checkpoint, or other means that are appropriate to the research performed.
- While NeurIPS does not require releasing code, the conference does require all submissions to provide some reasonable avenue for reproducibility, which may depend on the nature of the contribution. For example
 - (a) If the contribution is primarily a new algorithm, the paper should make it clear how to reproduce that algorithm.
 - (b) If the contribution is primarily a new model architecture, the paper should describe the architecture clearly and fully.
 - (c) If the contribution is a new model (e.g., a large language model), then there should either be a way to access this model for reproducing the results or a way to reproduce the model (e.g., with an open-source dataset or instructions for how to construct the dataset).
 - (d) We recognize that reproducibility may be tricky in some cases, in which case authors are welcome to describe the particular way they provide for reproducibility. In the case of closed-source models, it may be that access to the model is limited in some way (e.g., to registered users), but it should be possible for other researchers to have some path to reproducing or verifying the results.

5. Open access to data and code

Question: Does the paper provide open access to the data and code, with sufficient instructions to faithfully reproduce the main experimental results, as described in supplemental material?

Answer: [Yes]

Justification: We use open datasets, which have been cited and described in the paper. We will provide our code for reproducing the experimental results in the supplementary material.

Guidelines:

- The answer NA means that paper does not include experiments requiring code.
- Please see the NeurIPS code and data submission guidelines (<https://nips.cc/public/guides/CodeSubmissionPolicy>) for more details.
- While we encourage the release of code and data, we understand that this might not be possible, so “No” is an acceptable answer. Papers cannot be rejected simply for not including code, unless this is central to the contribution (e.g., for a new open-source benchmark).
- The instructions should contain the exact command and environment needed to run to reproduce the results. See the NeurIPS code and data submission guidelines (<https://nips.cc/public/guides/CodeSubmissionPolicy>) for more details.
- The authors should provide instructions on data access and preparation, including how to access the raw data, preprocessed data, intermediate data, and generated data, etc.
- The authors should provide scripts to reproduce all experimental results for the new proposed method and baselines. If only a subset of experiments are reproducible, they should state which ones are omitted from the script and why.
- At submission time, to preserve anonymity, the authors should release anonymized versions (if applicable).

- Providing as much information as possible in supplemental material (appended to the paper) is recommended, but including URLs to data and code is permitted.

6. Experimental setting/details

Question: Does the paper specify all the training and test details (e.g., data splits, hyper-parameters, how they were chosen, type of optimizer, etc.) necessary to understand the results?

Answer: [\[Yes\]](#)

Justification: We provide detailed experimental settings in the Experiment section and in Appendix.

Guidelines:

- The answer NA means that the paper does not include experiments.
- The experimental setting should be presented in the core of the paper to a level of detail that is necessary to appreciate the results and make sense of them.
- The full details can be provided either with the code, in appendix, or as supplemental material.

7. Experiment statistical significance

Question: Does the paper report error bars suitably and correctly defined or other appropriate information about the statistical significance of the experiments?

Answer: [\[Yes\]](#)

Justification: We report the error bar for averaging multiple seeds in our experiments.

Guidelines:

- The answer NA means that the paper does not include experiments.
- The authors should answer "Yes" if the results are accompanied by error bars, confidence intervals, or statistical significance tests, at least for the experiments that support the main claims of the paper.
- The factors of variability that the error bars are capturing should be clearly stated (for example, train/test split, initialization, random drawing of some parameter, or overall run with given experimental conditions).
- The method for calculating the error bars should be explained (closed form formula, call to a library function, bootstrap, etc.)
- The assumptions made should be given (e.g., Normally distributed errors).
- It should be clear whether the error bar is the standard deviation or the standard error of the mean.
- It is OK to report 1-sigma error bars, but one should state it. The authors should preferably report a 2-sigma error bar than state that they have a 96% CI, if the hypothesis of Normality of errors is not verified.
- For asymmetric distributions, the authors should be careful not to show in tables or figures symmetric error bars that would yield results that are out of range (e.g. negative error rates).
- If error bars are reported in tables or plots, The authors should explain in the text how they were calculated and reference the corresponding figures or tables in the text.

8. Experiments compute resources

Question: For each experiment, does the paper provide sufficient information on the computer resources (type of compute workers, memory, time of execution) needed to reproduce the experiments?

Answer: [\[Yes\]](#)

Justification: We provide the information on our computational resources in Appendix.

Guidelines:

- The answer NA means that the paper does not include experiments.
- The paper should indicate the type of compute workers CPU or GPU, internal cluster, or cloud provider, including relevant memory and storage.

- The paper should provide the amount of compute required for each of the individual experimental runs as well as estimate the total compute.
- The paper should disclose whether the full research project required more compute than the experiments reported in the paper (e.g., preliminary or failed experiments that didn't make it into the paper).

9. Code of ethics

Question: Does the research conducted in the paper conform, in every respect, with the NeurIPS Code of Ethics <https://neurips.cc/public/EthicsGuidelines>?

Answer: [Yes]

Justification: Our paper conform to every aspect in the NeurIPS Code of Ethics.

Guidelines:

- The answer NA means that the authors have not reviewed the NeurIPS Code of Ethics.
- If the authors answer No, they should explain the special circumstances that require a deviation from the Code of Ethics.
- The authors should make sure to preserve anonymity (e.g., if there is a special consideration due to laws or regulations in their jurisdiction).

10. Broader impacts

Question: Does the paper discuss both potential positive societal impacts and negative societal impacts of the work performed?

Answer: [No]

Justification: This paper presents work whose goal is to advance the field of Machine Learning. There are many potential societal consequences of our work, none which we feel must be specifically highlighted here.

Guidelines:

- The answer NA means that there is no societal impact of the work performed.
- If the authors answer NA or No, they should explain why their work has no societal impact or why the paper does not address societal impact.
- Examples of negative societal impacts include potential malicious or unintended uses (e.g., disinformation, generating fake profiles, surveillance), fairness considerations (e.g., deployment of technologies that could make decisions that unfairly impact specific groups), privacy considerations, and security considerations.
- The conference expects that many papers will be foundational research and not tied to particular applications, let alone deployments. However, if there is a direct path to any negative applications, the authors should point it out. For example, it is legitimate to point out that an improvement in the quality of generative models could be used to generate deepfakes for disinformation. On the other hand, it is not needed to point out that a generic algorithm for optimizing neural networks could enable people to train models that generate Deepfakes faster.
- The authors should consider possible harms that could arise when the technology is being used as intended and functioning correctly, harms that could arise when the technology is being used as intended but gives incorrect results, and harms following from (intentional or unintentional) misuse of the technology.
- If there are negative societal impacts, the authors could also discuss possible mitigation strategies (e.g., gated release of models, providing defenses in addition to attacks, mechanisms for monitoring misuse, mechanisms to monitor how a system learns from feedback over time, improving the efficiency and accessibility of ML).

11. Safeguards

Question: Does the paper describe safeguards that have been put in place for responsible release of data or models that have a high risk for misuse (e.g., pretrained language models, image generators, or scraped datasets)?

Answer: [NA]

Justification: There are no potential harms to our models.

Guidelines:

- The answer NA means that the paper poses no such risks.
- Released models that have a high risk for misuse or dual-use should be released with necessary safeguards to allow for controlled use of the model, for example by requiring that users adhere to usage guidelines or restrictions to access the model or implementing safety filters.
- Datasets that have been scraped from the Internet could pose safety risks. The authors should describe how they avoided releasing unsafe images.
- We recognize that providing effective safeguards is challenging, and many papers do not require this, but we encourage authors to take this into account and make a best faith effort.

12. Licenses for existing assets

Question: Are the creators or original owners of assets (e.g., code, data, models), used in the paper, properly credited and are the license and terms of use explicitly mentioned and properly respected?

Answer: [\[Yes\]](#)

Justification: We cite all data, code, and models used properly.

Guidelines:

- The answer NA means that the paper does not use existing assets.
- The authors should cite the original paper that produced the code package or dataset.
- The authors should state which version of the asset is used and, if possible, include a URL.
- The name of the license (e.g., CC-BY 4.0) should be included for each asset.
- For scraped data from a particular source (e.g., website), the copyright and terms of service of that source should be provided.
- If assets are released, the license, copyright information, and terms of use in the package should be provided. For popular datasets, paperswithcode.com/datasets has curated licenses for some datasets. Their licensing guide can help determine the license of a dataset.
- For existing datasets that are re-packaged, both the original license and the license of the derived asset (if it has changed) should be provided.
- If this information is not available online, the authors are encouraged to reach out to the asset's creators.

13. New assets

Question: Are new assets introduced in the paper well documented and is the documentation provided alongside the assets?

Answer: [\[NA\]](#)

Justification: We do not release new assets.

Guidelines:

- The answer NA means that the paper does not release new assets.
- Researchers should communicate the details of the dataset/code/model as part of their submissions via structured templates. This includes details about training, license, limitations, etc.
- The paper should discuss whether and how consent was obtained from people whose asset is used.
- At submission time, remember to anonymize your assets (if applicable). You can either create an anonymized URL or include an anonymized zip file.

14. Crowdsourcing and research with human subjects

Question: For crowdsourcing experiments and research with human subjects, does the paper include the full text of instructions given to participants and screenshots, if applicable, as well as details about compensation (if any)?

Answer: [NA]

Justification: Our paper does not involve crowdsourcing nor research with human subjects.

Guidelines:

- The answer NA means that the paper does not involve crowdsourcing nor research with human subjects.
- Including this information in the supplemental material is fine, but if the main contribution of the paper involves human subjects, then as much detail as possible should be included in the main paper.
- According to the NeurIPS Code of Ethics, workers involved in data collection, curation, or other labor should be paid at least the minimum wage in the country of the data collector.

15. Institutional review board (IRB) approvals or equivalent for research with human subjects

Question: Does the paper describe potential risks incurred by study participants, whether such risks were disclosed to the subjects, and whether Institutional Review Board (IRB) approvals (or an equivalent approval/review based on the requirements of your country or institution) were obtained?

Answer: [NA]

Justification: Our paper does not pose any potential risks to participants.

Guidelines:

- The answer NA means that the paper does not involve crowdsourcing nor research with human subjects.
- Depending on the country in which research is conducted, IRB approval (or equivalent) may be required for any human subjects research. If you obtained IRB approval, you should clearly state this in the paper.
- We recognize that the procedures for this may vary significantly between institutions and locations, and we expect authors to adhere to the NeurIPS Code of Ethics and the guidelines for their institution.
- For initial submissions, do not include any information that would break anonymity (if applicable), such as the institution conducting the review.

16. Declaration of LLM usage

Question: Does the paper describe the usage of LLMs if it is an important, original, or non-standard component of the core methods in this research? Note that if the LLM is used only for writing, editing, or formatting purposes and does not impact the core methodology, scientific rigor, or originality of the research, declaration is not required.

Answer: [No]

Justification: We only use LLM for writing and editing purposes.

Guidelines:

- The answer NA means that the core method development in this research does not involve LLMs as any important, original, or non-standard components.
- Please refer to our LLM policy (<https://neurips.cc/Conferences/2025/LLM>) for what should or should not be described.

A Formal Proofs

A.1 Full Gradient Formulas & Useful Lemmas

From the setting, at iteration t , we can take the derivative with respect to the j -th filter $\mathbf{w}_j^{(t)}$ in the following three training schemes:

1. GD training on the augmented dataset via upsampling: Lemmas A.1, A.2.
2. GD training on the augmented dataset via synthetic generation: Lemmas A.3, A.4.
3. SAM and GD training on the original dataset: Lemmas A.5, A.6.

Recall that k is the augmenting factor, and the augmented datasets D_G, D_U now have size $N_{\text{new}} = \alpha N + k(1 - \alpha)N$.

Lemma A.1. (*Upsampling: full gradient*) *In the augmented dataset D_U after upsampling the “slow-learnable” subset with a factor k , for $t \geq 0$ and $j \in [J]$, the gradient of the loss $\mathcal{L}^U(\mathbf{W}^{(t)})$ with respect to $\mathbf{w}_j^{(t)}$ is*

$$\begin{aligned} \nabla_{\mathbf{w}_j^{(t)}}^U \mathcal{L}(\mathbf{W}^{(t)}) = & -\frac{3}{N_{\text{new}}} \sum_{i=1}^{\alpha N} l_i^{(t)} \left(\beta_e^3 \langle \mathbf{w}_j^{(t)}, \mathbf{v}_e \rangle^2 \mathbf{v}_e + y_i \langle \mathbf{w}_j^{(t)}, \boldsymbol{\xi}_i \rangle^2 \boldsymbol{\xi}_i \right) \\ & - \frac{3k}{N_{\text{new}}} \sum_{i=\alpha N+1}^N k l_i^{(t)} \left(\beta_d^3 \langle \mathbf{w}_j^{(t)}, \mathbf{v}_d \rangle^2 \mathbf{v}_d + y_i \langle \mathbf{w}_j^{(t)}, \boldsymbol{\xi}_i \rangle^2 \boldsymbol{\xi}_i \right), \end{aligned}$$

where $l_i^{(t)} = \text{sigmoid}(-y_i f(\mathbf{x}_i; \mathbf{W}^{(t)}))$ for the two-layer CNN model f .

Proof. We compute the gradient directly from the loss function:

$$\begin{aligned} \nabla_{\mathbf{w}_j^{(t)}}^U \mathcal{L}(\mathbf{W}^{(t)}) &= -\frac{1}{N_{\text{new}}} \sum_{i=1}^{N_{\text{new}}} \frac{\exp(-y_i f(\mathbf{x}_i; \mathbf{W}^{(t)}))}{1 + \exp(-y_i f(\mathbf{x}_i; \mathbf{W}^{(t)}))} y_i \nabla_{\mathbf{w}_j^{(t)}} f(\mathbf{x}_i; \mathbf{W}^{(t)}) \\ &= -\frac{3}{N_{\text{new}}} \sum_{i=1}^{N_{\text{new}}} l_i^{(t)} y_i \sum_{p=1}^P \langle \mathbf{w}_j^{(t)}, \mathbf{x}^{(p)} \rangle^3 \\ &= -\frac{3}{N_{\text{new}}} \sum_{i=1}^{\alpha N} l_i^{(t)} \left(\beta_e^3 \langle \mathbf{w}_j^{(t)}, \mathbf{v}_e \rangle^2 \mathbf{v}_e + y_i \langle \mathbf{w}_j^{(t)}, \boldsymbol{\xi}_i \rangle^2 \boldsymbol{\xi}_i \right) \\ &\quad - \frac{3}{N_{\text{new}}} \sum_{i=\alpha N+1}^{N_{\text{new}}} l_i^{(t)} \left(\beta_d^3 \langle \mathbf{w}_j^{(t)}, \mathbf{v}_d \rangle^2 \mathbf{v}_d + y_i \langle \mathbf{w}_j^{(t)}, \boldsymbol{\xi}_i \rangle^2 \boldsymbol{\xi}_i \right) \\ &= -\frac{3}{N_{\text{new}}} \sum_{i=1}^{\alpha N} l_i^{(t)} \left(\beta_e^3 \langle \mathbf{w}_j^{(t)}, \mathbf{v}_e \rangle^2 \mathbf{v}_e + y_i \langle \mathbf{w}_j^{(t)}, \boldsymbol{\xi}_i \rangle^2 \boldsymbol{\xi}_i \right) \\ &\quad - \frac{3k}{N_{\text{new}}} \sum_{i=\alpha N+1}^N l_i^{(t)} \left(\beta_d^3 \langle \mathbf{w}_j^{(t)}, \mathbf{v}_d \rangle^2 \mathbf{v}_d + y_i \langle \mathbf{w}_j^{(t)}, \boldsymbol{\xi}_i \rangle^2 \boldsymbol{\xi}_i \right) \end{aligned}$$

where the last step follows from the fact that there are k copies of the same subset in the upsampled portion of the data. \square

Lemma A.2. (*Upsampling: feature & noise gradients*) *In the same setting, $\nabla_{\mathbf{w}_j^{(t)}}^U \mathcal{L}(\mathbf{W}^{(t)})$ learns the features and noises as follows:*

1. *Fast-learnable feature gradient:*

$$\langle \nabla_{\mathbf{w}_j^{(t)}}^U \mathcal{L}(\mathbf{W}^{(t)}), \mathbf{v}_e \rangle = -\frac{3\beta_e^3}{N_{\text{new}}} \sum_{i=1}^{\alpha N} l_i^{(t)} \langle \mathbf{w}_j^{(t)}, \mathbf{v}_e \rangle^2$$

2. Slow-learnable feature gradient:

$$\langle \nabla_{\mathbf{w}_j^{(t)}}^U \mathcal{L}(\mathbf{W}^{(t)}), \mathbf{v}_d \rangle = -\frac{3k\beta_d^3}{N_{\text{new}}} \sum_{i=\alpha N+1}^N l_i^{(t)} \langle \mathbf{w}_j^{(t)}, \mathbf{v}_d \rangle^2$$

3. Noise gradient:

(a). For ξ_i , $i = 1, \dots, \alpha N$

$$\langle \nabla_{\mathbf{w}_j^{(t)}}^U \mathcal{L}(\mathbf{W}^{(t)}), \xi_i \rangle = -\frac{3}{N_{\text{new}}} l_i^{(t)} y_i \langle \mathbf{w}_j^{(t)}, \xi_i \rangle^2 \|\xi_i\|^2.$$

(b). For ξ_i , $i = \alpha N + 1, \dots, N$

$$\langle \nabla_{\mathbf{w}_j^{(t)}}^U \mathcal{L}(\mathbf{W}^{(t)}), \xi_i \rangle = -\frac{3k}{N_{\text{new}}} l_i^{(t)} y_i \langle \mathbf{w}_j^{(t)}, \xi_i \rangle^2 \|\xi_i\|^2$$

Proof. The proof follows directly from taking the inner product with the gradient formula in Lemma A.1. Then we proceed using that $\mathbf{v}_e, \mathbf{v}_d, \xi_i$ form a orthogonal set and that summations involving noise cross-terms become negligible. \square

Lemma A.3. (Generation: full gradient) In the augmented dataset D_G after synthetically generating the “slow-learnable” subset with a factor k , for $t \geq 0$ and $j \in [J]$, the gradient of the loss $\mathcal{L}^G(\mathbf{W}^{(t)})$ with respect to $\mathbf{w}_j^{(t)}$ is

$$\begin{aligned} \nabla_{\mathbf{w}_j^{(t)}}^U \mathcal{L}(\mathbf{W}^{(t)}) &= -\frac{3}{N_{\text{new}}} \sum_{i=1}^{\alpha N} l_i^{(t)} \left(\beta_e^3 \langle \mathbf{w}_j^{(t)}, \mathbf{v}_e \rangle^2 \mathbf{v}_e + y_i \langle \mathbf{w}_j^{(t)}, \xi_i \rangle^2 \xi_i \right) \\ &\quad - \frac{3}{N_{\text{new}}} \sum_{i=\alpha N+1}^N l_i^{(t)} \left(\beta_d^3 \langle \mathbf{w}_j^{(t)}, \mathbf{v}_d \rangle^2 \mathbf{v}_d + y_i \langle \mathbf{w}_j^{(t)}, \xi_i \rangle^2 \xi_i \right) \\ &\quad - \frac{3}{N_{\text{new}}} \sum_{i=N+1}^{N_{\text{new}}} l_i^{(t)} \left(\beta_d^3 \langle \mathbf{w}_j^{(t)}, \mathbf{v}_d \rangle^2 \mathbf{v}_d + y_i \langle \mathbf{w}_j^{(t)}, \gamma_i \rangle^2 \gamma_i \right), \end{aligned}$$

where $l_i^{(t)} = \text{sigmoid}(-y_i f(\mathbf{x}_i; \mathbf{W}^{(t)}))$ for the two-layer CNN model f .

Proof. The proof is similar to that of Lemma A.1, except that for data that contain \mathbf{v}_d , the first $(1 - \alpha)N$ data points come from the original dataset, and the rest comes from synthetic generation with noise γ_i , $i = N + 1, \dots, N_{\text{new}}$. \square

Lemma A.4. (Generation: feature & noise gradients) In the same setting, $\nabla_{\mathbf{w}_j^{(t)}}^G \mathcal{L}(\mathbf{W}^{(t)})$ learns the features and noises as follows:

1. Fast-learnable feature gradient:

$$\langle \nabla_{\mathbf{w}_j^{(t)}}^G \mathcal{L}(\mathbf{W}^{(t)}), \mathbf{v}_e \rangle = -\frac{3\beta_e^3}{N_{\text{new}}} \sum_{i=1}^{\alpha N} l_i^{(t)} \langle \mathbf{w}_j^{(t)}, \mathbf{v}_e \rangle^2$$

2. Slow-learnable feature gradient:

$$\langle \nabla_{\mathbf{w}_j^{(t)}}^G \mathcal{L}(\mathbf{W}^{(t)}), \mathbf{v}_d \rangle = -\frac{3\beta_d^3}{N_{\text{new}}} \sum_{i=\alpha N+1}^{N_{\text{new}}} l_i^{(t)} \langle \mathbf{w}_j^{(t)}, \mathbf{v}_d \rangle^2$$

3. **Noise gradient:** Let $\{\phi_i\}_{i=1}^{N_{\text{new}}} = \{\xi_i\}_{i=1}^N \cup \{\gamma_i\}_{i=N+1}^{N_{\text{new}}}$ denote the set of noises in D_G (which can be the original or generation noise). Then for any ϕ_i , $i \in [N_{\text{new}}]$,

$$\langle \nabla_{\mathbf{w}_j^{(t)}}^G \mathcal{L}(\mathbf{W}^{(t)}), \phi_i \rangle = -\frac{3}{N_{\text{new}}} l_i^{(t)} y_i \langle \mathbf{w}_j^{(t)}, \phi_i \rangle^2 \|\phi_i\|^2.$$

Proof. Similar to Lemma A.2. We directly take the inner product and assume that all the noises are dispersed such that summations involving their cross-terms become insignificant in high dimension. Recall we also assume that the generation noise is orthogonal to features and independent of ξ_i 's. \square

Following the same process, we have the following gradients for SAM and GD on the original dataset.

Lemma A.5. (Original dataset: SAM & GD gradients) In the original dataset D , for $t \geq 0$ and $j \in [J]$ of GD, the gradient of the loss $\mathcal{L}(\mathbf{W}^{(t)})$ with respect to $\mathbf{w}_j^{(t)}$ is

$$\begin{aligned} \nabla_{\mathbf{w}_j^{(t)}} \mathcal{L}(\mathbf{W}^{(t)}) &= -\frac{3}{N} \sum_{i=1}^{\alpha N} l_i^{(t)} \left(\beta_e^3 \langle \mathbf{w}_j^{(t)}, \mathbf{v}_e \rangle^2 \mathbf{v}_e + y_i \langle \mathbf{w}_j^{(t)}, \xi_i \rangle^2 \xi_i \right) \\ &\quad - \frac{3}{N} \sum_{i=\alpha N+1}^N l_i^{(t)} \left(\beta_d^3 \langle \mathbf{w}_j^{(t)}, \mathbf{v}_d \rangle^2 \mathbf{v}_d + y_i \langle \mathbf{w}_j^{(t)}, \xi_i \rangle^2 \xi_i \right), \end{aligned}$$

where $l_i^{(t)} = \text{sigmoid}(-y_i f(\mathbf{x}_i; \mathbf{W}^{(t)}))$ for the two-layer CNN model f .

Suppose we train with SAM. Then the perturbed gradient has the same expression except that we replace $\mathbf{w}_j^{(t)}$ with the perturbed weights $\mathbf{w}_{j,\epsilon}^{(t)}$ and replace $l_i^{(t)}$ with $l_{i,\epsilon}^{(t)} = \text{sigmoid}(-y_i f(\mathbf{x}_i; \mathbf{W}^{(t)} + \epsilon^{(t)}))$:

$$\begin{aligned} \nabla_{\mathbf{w}_{j,\epsilon}^{(t)}} \mathcal{L}(\mathbf{W}^{(t)} + \epsilon^{(t)}) &= \nabla_{\mathbf{w}_{j,\epsilon}^{(t)}} \mathcal{L} \left(\mathbf{W}^{(t)} + \frac{\rho}{\|\nabla(\mathcal{L}(\mathbf{W}^{(t)}))\|_F} \nabla(\mathcal{L}(\mathbf{W}^{(t)})) \right) \\ &= -\frac{3}{N} \sum_{i=1}^{\alpha N} l_{i,\epsilon}^{(t)} \left(\beta_e^3 \langle \mathbf{w}_{j,\epsilon}^{(t)}, \mathbf{v}_e \rangle^2 \mathbf{v}_e + y_i \langle \mathbf{w}_{j,\epsilon}^{(t)}, \xi_i \rangle^2 \xi_i \right) \\ &\quad - \frac{3}{N} \sum_{i=\alpha N+1}^N l_{i,\epsilon}^{(t)} \left(\beta_d^3 \langle \mathbf{w}_{j,\epsilon}^{(t)}, \mathbf{v}_d \rangle^2 \mathbf{v}_d + y_i \langle \mathbf{w}_{j,\epsilon}^{(t)}, \xi_i \rangle^2 \xi_i \right). \end{aligned}$$

Lemma A.6. (Original dataset: SAM & GD feature & noise gradients) In the same setting, $\nabla_{\mathbf{w}_j^{(t)}} \mathcal{L}(\mathbf{W}^{(t)})$ learns the features and noises as follows:

1. *Fast-learnable feature gradient:*

$$\langle \nabla_{\mathbf{w}_j^{(t)}} \mathcal{L}(\mathbf{W}^{(t)}), \mathbf{v}_e \rangle = -\frac{3\beta_e^3}{N} \sum_{i=1}^{\alpha N} l_i^{(t)} \langle \mathbf{w}_j^{(t)}, \mathbf{v}_e \rangle^2$$

2. *Slow-learnable feature gradient:*

$$\langle \nabla_{\mathbf{w}_j^{(t)}} \mathcal{L}(\mathbf{W}^{(t)}), \mathbf{v}_d \rangle = -\frac{3\beta_d^3}{N} \sum_{i=\alpha N+1}^N l_i^{(t)} \langle \mathbf{w}_j^{(t)}, \mathbf{v}_d \rangle^2$$

3. *Noise gradient:*

$$\langle \nabla_{\mathbf{w}_j^{(t)}} \mathcal{L}(\mathbf{W}^{(t)}), \xi_i \rangle = -\frac{3}{N} l_i^{(t)} y_i \langle \mathbf{w}_j^{(t)}, \xi_i \rangle^2 \|\xi_i\|^2.$$

The SAM feature & noise gradients are similar except that we replace $\mathbf{w}_j^{(t)}$, $l_i^{(t)}$ with $\mathbf{w}_{j,\epsilon}^{(t)}$, $l_{i,\epsilon}^{(t)}$.

Remark. Suppose the data point \mathbf{x}_i has feature \mathbf{v}_d and noise ϕ_i . We have that

$$\begin{aligned} l_i^{(t)} &= \text{sigmoid} \left(\sum_{j=1}^J -\beta_d^3 \langle \mathbf{w}_j^{(t)}, \mathbf{v}_d \rangle^3 - y_i \langle \mathbf{w}_j^{(t)}, \phi_i \rangle^3 \right), \\ \text{and } l_{i,\epsilon}^{(t)} &= \text{sigmoid} \left(\sum_{j=1}^J -\beta_d^3 \langle \mathbf{w}_{j,\epsilon}^{(t)}, \mathbf{v}_d \rangle^3 - y_i \langle \mathbf{w}_{j,\epsilon}^{(t)}, \phi_i \rangle^3 \right). \end{aligned} \tag{3}$$

The same formula holds if the feature is \mathbf{v}_e .

Insights from gradient formulas. By directly computing these relevant gradients, we can see that some observed phenomena already become self-explanatory in the formulas. For instance, Lemma A.2 implies that for upsampling, the gradient alignment is k times larger for the noises we replicated. At a high level, this would cause overfitting to these particular noises when performing gradient update. In the next section, we formalize the intuition by examining the underlying mechanism of noise learning in greater detail.

B GD vs. SAM Noise Learning: Proof of Theorem 4.1

Remark. Heuristically, we say that the noise is being learned well if the magnitude of the alignment $|\langle \mathbf{w}_j^{(t)}, \boldsymbol{\xi}_i \rangle|$ is large, meaning that the weights align or misalign with the noise to a great extent. We say that the model is learning the noise if $|\langle \mathbf{w}_j^{(t)}, \boldsymbol{\xi}_i \rangle|$ increases over time. In practice, overly fitting or overly avoiding certain noises are both harmful to a model's generalization.

Lemma B.1. (Gradient norm bound) *In our setting, we can bound the norm of the gradient matrix $\nabla \mathcal{L}(\mathbf{W}^{(t)})$ as:*

$$\|\nabla \mathcal{L}(\mathbf{W}^{(t)})\|_F \geq \frac{3}{N} l_i^{(t)} \langle \mathbf{w}_j^{(t)}, \boldsymbol{\xi}_i \rangle^2 \|\boldsymbol{\xi}_i\| \quad \forall i.$$

Proof. This norm can be lower bounded by the the norm of one column:

$$\begin{aligned} \|\nabla \mathcal{L}(\mathbf{W}^{(t)})\|_F &= \sqrt{\sum_{j=1}^J \left\| \nabla_{\mathbf{w}_j^{(t)}} \mathcal{L}(\mathbf{W}^{(t)}) \right\|^2} \\ &\geq \left\| \nabla_{\mathbf{w}_j^{(t)}} \mathcal{L}(\mathbf{W}^{(t)}) \right\| \quad \text{for some neuron } j \\ &= \sqrt{\frac{9\beta_e^6}{N^2} \langle \mathbf{w}_j^{(t)}, \mathbf{v}_e \rangle^4 \left(\sum_{i=1}^{\alpha N} l_i^{(t)} \right)^2 + \frac{9\beta_d^6}{N^2} \langle \mathbf{w}_j^{(t)}, \mathbf{v}_d \rangle^4 \left(\sum_{i=\alpha N+1}^N l_i^{(t)} \right)^2 + \left\| \frac{3}{N} \sum_{i=1}^N l_i^{(t)} y_i \langle \mathbf{w}_j^{(t)}, \boldsymbol{\xi}_i \rangle^2 \boldsymbol{\xi}_i \right\|^2} \\ &\quad \text{by taking the norm of the gradient in Lemma A.5 and using orthogonality} \\ &\geq \left\| \frac{3}{N} \sum_{i=1}^N l_i^{(t)} y_i \langle \mathbf{w}_j^{(t)}, \boldsymbol{\xi}_i \rangle^2 \boldsymbol{\xi}_i \right\| \geq \left\| \frac{3}{N} l_i^{(t)} y_i \langle \mathbf{w}_j^{(t)}, \boldsymbol{\xi}_i \rangle^2 \boldsymbol{\xi}_i \right\| = \frac{3}{N} l_i^{(t)} \langle \mathbf{w}_j^{(t)}, \boldsymbol{\xi}_i \rangle^2 \|\boldsymbol{\xi}_i\| \quad \forall i \\ &\quad \text{since cross terms become negligible} \end{aligned}$$

□

Lemma B.2. (Noise set equivalences) *With a sufficiently small SAM perturbation parameter ρ , at some early iteration t , the following set relations hold:*

$$\mathcal{I}_{j,+}^{(t)} = \mathcal{I}_{j,\epsilon,+}^{(t)}, \quad \mathcal{I}_{j,-}^{(t)} = \mathcal{I}_{j,\epsilon,-}^{(t)}.$$

Proof. We first note that for some early training weights $\mathbf{W}^{(t)}$, we have the following connection between the original weights and the SAM perturbed weights:

$$\begin{aligned} \langle \mathbf{w}_{j,\epsilon}^{(t)}, \boldsymbol{\xi}_i \rangle &= \langle \mathbf{w}_j^{(t)} + \rho^{(t)} \nabla_{\mathbf{w}_j^{(t)}} \mathcal{L}(\mathbf{W}^{(t)}), \boldsymbol{\xi}_i \rangle \\ &= \langle \mathbf{w}_j^{(t)}, \boldsymbol{\xi}_i \rangle + \rho^{(t)} \langle \nabla_{\mathbf{w}_j^{(t)}} \mathcal{L}(\mathbf{W}^{(t)}), \boldsymbol{\xi}_i \rangle \\ &= \langle \mathbf{w}_j^{(t)}, \boldsymbol{\xi}_i \rangle - \frac{3\rho^{(t)}}{N} l_i^{(t)} y_i \langle \mathbf{w}_j^{(t)}, \boldsymbol{\xi}_i \rangle^2 \|\boldsymbol{\xi}_i\|^2 \quad \text{by Lemma A.6} \end{aligned} \tag{4}$$

We consider sufficiently small ρ such that:

$$0 < \rho < \min \left\{ \frac{|\langle \mathbf{w}_j^{(t)}, \boldsymbol{\xi}_i \rangle|}{\|\boldsymbol{\xi}_i\|} : \boldsymbol{\xi}_i \in D \right\}. \tag{5}$$

We recall that $\rho^{(t)} = \rho / \|\nabla \mathcal{L}(\mathbf{W}^{(t)})\|_F$. Then suppose $\xi_i \in \mathcal{I}_{j,-}^{(t)}$, that is y_i and $\langle \mathbf{w}_j^{(t)}, \xi_i \rangle$ have opposite signs. Eq. 4 implies

$$\begin{aligned} \langle \mathbf{w}_{j,\epsilon}^{(t)}, \xi_i \rangle &= \langle \mathbf{w}_j^{(t)}, \xi_i \rangle \left(1 - \frac{3\rho^{(t)}}{N} l_i^{(t)} y_i \langle \mathbf{w}_j^{(t)}, \xi_i \rangle \|\xi_i\|^2 \right) \\ &= \underbrace{\langle \mathbf{w}_j^{(t)}, \xi_i \rangle \left(1 + \frac{3\rho^{(t)}}{N} l_i^{(t)} \|\xi_i\|^2 |\langle \mathbf{w}_j^{(t)}, \xi_i \rangle| \right)}_{>0}, \end{aligned}$$

which implies that $\text{sgn}(\langle \mathbf{w}_{j,\epsilon}^{(t)}, \xi_i \rangle) = \text{sgn}(\langle \mathbf{w}_j^{(t)}, \xi_i \rangle)$ and $\xi_i \in \mathcal{I}_{j,\epsilon,-}^{(t)}$.

Now suppose $\xi_i \in \mathcal{I}_{j,+}^{(t)}$. Eq. 4 becomes:

$$\begin{aligned} \langle \mathbf{w}_{j,\epsilon}^{(t)}, \xi_i \rangle &= \langle \mathbf{w}_j^{(t)}, \xi_i \rangle \left(1 - \frac{3\rho^{(t)}}{N} l_i^{(t)} y_i \langle \mathbf{w}_j^{(t)}, \xi_i \rangle \|\xi_i\|^2 \right) \\ &= \underbrace{\langle \mathbf{w}_j^{(t)}, \xi_i \rangle \left(1 - \frac{3\rho^{(t)}}{N} l_i^{(t)} \|\xi_i\|^2 |\langle \mathbf{w}_j^{(t)}, \xi_i \rangle| \right)}_{\in (0, 1) \text{ as shown below}} \end{aligned}$$

Note that Lemma B.1 gives us:

$$\begin{aligned} 1 > 1 - \frac{3\rho^{(t)}}{N} l_i^{(t)} \|\xi_i\|^2 |\langle \mathbf{w}_j^{(t)}, \xi_i \rangle| &= 1 - \frac{3}{N} \frac{\rho}{\|\nabla \mathcal{L}(\mathbf{W}^{(t)})\|_F} l_i^{(t)} \|\xi_i\|^2 |\langle \mathbf{w}_j^{(t)}, \xi_i \rangle| \\ &\geq 1 - \frac{3}{N} \frac{\rho}{\frac{3}{N} l_i^{(t)} \langle \mathbf{w}_j^{(t)}, \xi_i \rangle^2 \|\xi_i\|} l_i^{(t)} \|\xi_i\|^2 |\langle \mathbf{w}_j^{(t)}, \xi_i \rangle| \\ &= 1 - \frac{\rho \|\xi_i\|}{|\langle \mathbf{w}_j^{(t)}, \xi_i \rangle|} \\ &> 1 - \frac{|\langle \mathbf{w}_j^{(t)}, \xi_i \rangle|}{\|\xi_i\|} \frac{\|\xi_i\|}{|\langle \mathbf{w}_j^{(t)}, \xi_i \rangle|} \quad \text{by the choice of } \rho \\ &= 0. \end{aligned} \tag{6}$$

Hence, we have that $\text{sgn}(\langle \mathbf{w}_{j,\epsilon}^{(t)}, \xi_i \rangle) = \text{sgn}(\langle \mathbf{w}_j^{(t)}, \xi_i \rangle)$ and $\xi_i \in \mathcal{I}_{j,\epsilon,+}^{(t)}$. Since $\mathcal{I}_{j,+}^{(t)}$ and $\mathcal{I}_{j,-}^{(t)}$ cover all the noises, the lemma statement follows. \square

B.1 Proof of Theorem 4.1.

We then start with item (1) of the theorem. First, for GD, each noise update is computed via:

$$\begin{aligned} \langle \mathbf{w}_j^{(t+1)}, \xi_i \rangle &= \langle \mathbf{w}_j^{(t)}, \xi_i \rangle - \eta \langle \nabla_{\mathbf{w}_j^{(t)}} \mathcal{L}(\mathbf{W}^{(t)}), \xi_i \rangle \\ &= \langle \mathbf{w}_j^{(t)}, \xi_i \rangle + \frac{3\eta}{N} l_i^{(t)} y_i \langle \mathbf{w}_j^{(t)}, \xi_i \rangle^2 \|\xi_i\|^2 \quad \text{by Lemma A.6} \\ &= \langle \mathbf{w}_j^{(t)}, \xi_i \rangle \left(1 + \eta \frac{3}{N} l_i^{(t)} y_i \|\xi_i\|^2 |\langle \mathbf{w}_j^{(t)}, \xi_i \rangle| \right) \end{aligned} \tag{7}$$

Then by definition, for all the noises $\xi_i \in \mathcal{I}_{j,-}^{(t)}$, y_i and $\langle \mathbf{w}_j^{(t)}, \xi_i \rangle$ have opposite signs, so the above equation becomes:

$$\langle \mathbf{w}_j^{(t+1)}, \xi_i \rangle = \langle \mathbf{w}_j^{(t)}, \xi_i \rangle \left(1 - \eta \frac{3}{N} l_i^{(t)} \|\xi_i\|^2 |\langle \mathbf{w}_j^{(t)}, \xi_i \rangle| \right).$$

With loss of generality, we consider the case when $\langle \mathbf{w}_j^{(t)}, \xi_i \rangle > 0$. We then define the corresponding sequence $a_t = \langle \mathbf{w}_j^{(t)}, \xi_i \rangle$ generated by the update:

$$a_{t+1} = a_t (1 - \eta C_i l_i^{(t)} a_t), \quad \text{where } C_i = \frac{3}{N} \|\xi_i\|^2.$$

Next, we want to show that given a proper η , this sequence is monotonic towards 0, meaning that these noises are gradually “unlearned” by the weights. We provide an inductive step below, which can be easily generalized.

If the learning rate satisfies

$$0 < \eta < \frac{1}{C_i a_t} = \frac{1}{C_i \langle \mathbf{w}_j^{(t)}, \boldsymbol{\xi}_i \rangle},$$

then by the update, the following inequality holds:

$$0 < a_t \left(1 - \frac{1}{C_i a_t} C_i l_i^{(t)} a_t \right) = a_t (1 - l_i^{(t)}) < a_{t+1} < a_t$$

Consequently, $a_{t+1} < a_t$ implies that

$$\eta < \frac{1}{C_i a_t} < \frac{1}{C_i a_{t+1}} \implies a_{t+2} < a_{t+1} \quad \text{by the same argument.}$$

A similar argument holds for $\langle \mathbf{w}_j^{(t)}, \boldsymbol{\xi}_i \rangle < 0$. Hence, if we take sufficiently small

$$\eta < \min \left\{ \frac{1}{C_i |\langle \mathbf{w}_j^{(t)}, \boldsymbol{\xi}_i \rangle|} : \boldsymbol{\xi}_i \in \mathcal{I}_{j,-}^{(t)} \right\},$$

the weights’ alignment with these noises will be monotonic throughout the updates and get closer and closer to 0. The proof for SAM is similar (we replace $\langle \mathbf{w}_j^{(t)}, \boldsymbol{\xi}_i \rangle$ by $\langle \mathbf{w}_{j,\epsilon}^{(t)}, \boldsymbol{\xi}_i \rangle$ for $\boldsymbol{\xi}_i \in \mathcal{I}_{j,\epsilon,-}^{(t)}$, etc.).

Now we proceed with item (2).

Then we consider $\boldsymbol{\xi}_i \in \mathcal{I}_{j,+}^{(t)} = \mathcal{I}_{j,\epsilon,+}^{(t)}$ in the setting of Lemma B.2. Eq. 7 now becomes:

$$\begin{aligned} \langle \mathbf{w}_j^{(t+1)}, \boldsymbol{\xi}_i \rangle &= \langle \mathbf{w}_j^{(t)}, \boldsymbol{\xi}_i \rangle \left(1 + \eta \frac{3}{N} l_i^{(t)} y_i \|\boldsymbol{\xi}_i\|^2 \langle \mathbf{w}_j^{(t)}, \boldsymbol{\xi}_i \rangle \right) \\ &= \langle \mathbf{w}_j^{(t)}, \boldsymbol{\xi}_i \rangle \left(1 + \eta \frac{3}{N} l_i^{(t)} \|\boldsymbol{\xi}_i\|^2 |\langle \mathbf{w}_j^{(t)}, \boldsymbol{\xi}_i \rangle| \right) \implies |\langle \mathbf{w}_j^{(t+1)}, \boldsymbol{\xi}_i \rangle| > |\langle \mathbf{w}_j^{(t)}, \boldsymbol{\xi}_i \rangle|. \end{aligned} \quad (8)$$

And a similar expression holds for SAM. Consequently, the alignments will be monotonically away from 0, continually being learned through iterations. Hence, we want to compare how the gradients align with noises: $|\langle \nabla_{\mathbf{w}_{j,\epsilon}} \mathcal{L}(\mathbf{W}^{(t)} + \boldsymbol{\epsilon}^{(t)}), \boldsymbol{\xi}_i \rangle|$ vs. $|\langle \nabla_{\mathbf{w}_j} \mathcal{L}(\mathbf{W}^{(t)}), \boldsymbol{\xi}_i \rangle|$. By Lemma A.6, we have that

$$\text{For } \mathbf{GD}: \quad |\langle \nabla_{\mathbf{w}_j} \mathcal{L}(\mathbf{W}^{(t)}), \boldsymbol{\xi}_i \rangle| = \frac{3}{N} l_i^{(t)} \langle \mathbf{w}_j^{(t)}, \boldsymbol{\xi}_i \rangle^2 \|\boldsymbol{\xi}_i\|^2.$$

$$\begin{aligned} \text{For } \mathbf{SAM}: \quad |\langle \nabla_{\mathbf{w}_{j,\epsilon}} \mathcal{L}(\mathbf{W}^{(t)} + \boldsymbol{\epsilon}^{(t)}), \boldsymbol{\xi}_i \rangle| &= \frac{3}{N} l_{i,\epsilon}^{(t)} \langle \mathbf{w}_{j,\epsilon}^{(t)}, \boldsymbol{\xi}_i \rangle^2 \|\boldsymbol{\xi}_i\|^2 \\ &\stackrel{(i)}{=} \frac{3}{N} l_{i,\epsilon}^{(t)} \left(\langle \mathbf{w}_j^{(t)}, \boldsymbol{\xi}_i \rangle - \frac{3\rho^{(t)}}{N} l_i^{(t)} y_i \langle \mathbf{w}_j^{(t)}, \boldsymbol{\xi}_i \rangle^2 \|\boldsymbol{\xi}_i\|^2 \right)^2 \|\boldsymbol{\xi}_i\|^2 \\ &= \frac{3}{N} l_{i,\epsilon}^{(t)} \langle \mathbf{w}_j^{(t)}, \boldsymbol{\xi}_i \rangle^2 \left(1 - \frac{3\rho^{(t)}}{N} l_i^{(t)} y_i \langle \mathbf{w}_j^{(t)}, \boldsymbol{\xi}_i \rangle \|\boldsymbol{\xi}_i\|^2 \right)^2 \|\boldsymbol{\xi}_i\|^2 \\ &\stackrel{(ii)}{=} \frac{3}{N} l_i^{(t)} \langle \mathbf{w}_j^{(t)}, \boldsymbol{\xi}_i \rangle^2 \left(1 - \frac{3\rho^{(t)}}{N} l_i^{(t)} \|\boldsymbol{\xi}_i\|^2 |\langle \mathbf{w}_j^{(t)}, \boldsymbol{\xi}_i \rangle| \right)^2 \|\boldsymbol{\xi}_i\|^2, \end{aligned} \quad (9)$$

where (i) follows from Eq. 4 and (ii) is similar to [30], which claims that we can use the approximation for the logits in early training ($l_i^{(t)} = l_{i,\epsilon}^{(t)}$, see proof of their Lemma A.17). Now with a sufficiently small ρ that satisfies Eq. 3, the bound in 6 yields

$$\begin{aligned} |\langle \nabla_{\mathbf{w}_{j,\epsilon}} \mathcal{L}(\mathbf{W}^{(t)} + \boldsymbol{\epsilon}^{(t)}), \boldsymbol{\xi}_i \rangle| &= \frac{3}{N} l_i^{(t)} \underbrace{\langle \mathbf{w}_j^{(t)}, \boldsymbol{\xi}_i \rangle^2 \left(1 - \frac{3\rho^{(t)}}{N} l_i^{(t)} \|\boldsymbol{\xi}_i\|^2 |\langle \mathbf{w}_j^{(t)}, \boldsymbol{\xi}_i \rangle| \right)^2}_{\in (0,1)} \|\boldsymbol{\xi}_i\|^2 \\ &< \frac{3}{N} l_i^{(t)} \langle \mathbf{w}_j^{(t)}, \boldsymbol{\xi}_i \rangle^2 \|\boldsymbol{\xi}_i\|^2 = |\langle \nabla_{\mathbf{w}_j} \mathcal{L}(\mathbf{W}^{(t)}), \boldsymbol{\xi}_i \rangle|. \end{aligned}$$

Since this inequality holds for all $\xi_i \in \mathcal{I}_{j,+}^{(t)} = \mathcal{I}_{j,\epsilon,+}^{(t)}$, we compute the average over these noises and have that:

$$\text{NoiseAlign}(\mathcal{I}_{j,\epsilon,+}^{(t)}, \mathbf{w}_{j,\epsilon}^{(t)}) = \text{NoiseAlign}(\mathcal{I}_{j,+}^{(t)}, \mathbf{w}_{j,\epsilon}^{(t)}) < \text{NoiseAlign}(\mathcal{I}_{j,+}^{(t)}, \mathbf{w}_j^{(t)}).$$

The special case of the theorem can be proved by directly setting the early training weights to be the initialization $\mathbf{W}^{(0)}$. Since $\mathbf{W}^{(0)} \sim \mathcal{N}(0, \sigma_0^2)$ and $\xi_i \sim \mathcal{N}(0, \sigma_p^2/d)$, with a large N , $\mathcal{I}_{j,+}^{(0)}$ and $\mathcal{I}_{j,-}^{(0)}$ will each contain roughly half of the noises, as $\text{sgn}(\langle \mathbf{w}_{j,\epsilon}^{(0)}, \xi_i \rangle) = \text{sgn}(y_i)$ has probability 0.5 in this case.

Remark. The theory matches our insights that the noises tend to be fitted in general for the upsampled dataset. We do note that the bound in Lemma B.1 can be loose, as it covers very extreme cases, and the actual choice of ρ could be much larger in general without breaking the logic of our argument.

C Generation vs. Upsampling: Bias Perspective and Proof of Theorem 4.2

Item (1) of this theorem can be proved in a similar fashion as for Theorem 4.1 in Appendix B.

For item (2), the update rules follow directly from Lemmas A.2, A.4. Again these formulas themselves can partially explain what happens: the “generation” gradient learns every noise in the same manner, but the “upsampling” gradient learns the replicated noises k times more in one iteration.

Lemma C.1. (*Static noise sets*) In our setting, with a sufficiently small learning rate ρ , for all $j \in [J]$ and all the early iterations $t = 0, \dots, T$, we have that:

$$\begin{aligned} \mathcal{I}_{j,+}^{G,(0)} &= \mathcal{I}_{j,+}^{G,(1)} = \dots = \mathcal{I}_{j,+}^{G,(t)} = \dots = \mathcal{I}_{j,+}^{G,(T)}, \\ \mathcal{I}_{j,+}^{U,(0)} &= \mathcal{I}_{j,+}^{U,(1)} = \dots = \mathcal{I}_{j,+}^{U,(t)} = \dots = \mathcal{I}_{j,+}^{U,(T)}. \end{aligned}$$

The same holds for the corresponding sets $\mathcal{I}_{j,-}^{G,(t)}$ and $\mathcal{I}_{j,-}^{U,(t)}$.

Proof. This directly follows from the previous proofs, where starting from the initializations, certain noise alignments move towards 0 and others move away from 0 early in training. Hence, in this process, the signs do not change, and these sets always contain the same noises as t progresses \square

We now focus on the informal special case and show that in expectation, our requirement on the generation noise prevents $\text{NoiseAlign}(\mathcal{I}_{j,+}^{G,(t)}, \mathbf{w}_j^{(t)})$ from getting too large. In particular, we assume that the number of neurons J is sufficiently large such that we can replace the noisy sigmoid logits with the noiseless version in Eq. 3:

$$l_i^{(t)} = \text{sigmoid} \left(\sum_{j=1}^J -\beta_d^3 \langle \mathbf{w}_j^{(t)}, \mathbf{v}_d \rangle^3 - y_i \langle \mathbf{w}_j^{(t)}, \phi_i \rangle^3 \right) \approx l_d^{(t)} := \text{sigmoid} \left(\sum_{j=1}^J -\beta_d^3 \langle \mathbf{w}_j^{(t)}, \mathbf{v}_d \rangle^3 \right)$$

or

$$l_i^{(t)} = \text{sigmoid} \left(\sum_{j=1}^J -\beta_e^3 \langle \mathbf{w}_j^{(t)}, \mathbf{v}_e \rangle^3 - y_i \langle \mathbf{w}_j^{(t)}, \phi_i \rangle^3 \right) \approx l_d^{(t)} := \text{sigmoid} \left(\sum_{j=1}^J -\beta_d^3 \langle \mathbf{w}_j^{(t)}, \mathbf{v}_e \rangle^3 \right)$$

depending on the feature. That is, the model has sufficient neurons J to average out the second term in summation.

In the theorem, we also assume N is sufficiently large such that the insights from expectation can be captured by the empirical quantity. In the following part, we (somewhat informally) use $\stackrel{E}{=}$, $\stackrel{E}{>}$ to indicate equality/inequality in expectation.

By our random initializations, we should again have $|\mathcal{I}_{j,+}^{G,(0)}| \approx |\mathcal{I}_{j,-}^{G,(0)}|$ and $|\mathcal{I}_{j,+}^{U,(0)}| \approx |\mathcal{I}_{j,-}^{U,(0)}|$, each randomly occupying around half of the noises. Lemma C.1 implies they continue to hold across early iterations. We now start with computing $\text{NoiseAlign}(\mathcal{I}_{j,+}^{G,(0)}, \mathbf{w}_j^{(0)})$: for simplicity, we let $\nabla_j(t) := \nabla_{\mathbf{w}_j^{(t)}} \mathcal{L}(\mathbf{W}^{(t)})$,

$$\begin{aligned}
& \frac{1}{|\mathcal{I}_{j,+}^{G,(0)}|} \left(\sum_{i=1, \xi_i \in \mathcal{I}_{j,+}^{G,(0)}}^N |\langle \nabla_j(0), \xi_i \rangle| + \sum_{i=N+1, \gamma_i \in \mathcal{I}_{j,+}^{G,(0)}}^{N_{\text{new}}} |\langle \nabla_j(0), \gamma_i \rangle| \right) \\
& \stackrel{E}{=} \frac{1}{|\mathcal{I}_{j,+}^{U,(0)}|} \left(\sum_{i=1, \xi_i \in \mathcal{I}_{j,+}^{G,(0)}}^{\alpha N} |\langle \nabla_j(0), \xi_i \rangle| + \sum_{i=\alpha N+1, \xi_i \in \mathcal{I}_{j,+}^{G,(0)}}^N |\langle \nabla_j(0), \xi_i \rangle| + \sum_{i=N+1, \gamma_i \in \mathcal{I}_{j,+}^{G,(0)}}^{N_{\text{new}}} |\langle \nabla_j(0), \gamma_i \rangle| \right) \quad (i) \\
& = \frac{1}{|\mathcal{I}_{j,+}^{U,(0)}|} \left(\sum_{i=1, \xi_i \in \mathcal{I}_{j,+}^{U,(0)}}^{\alpha N} |\langle \nabla_j(0), \xi_i \rangle| + \sum_{i=\alpha N+1, \xi_i \in \mathcal{I}_{j,+}^{U,(0)}}^N |\langle \nabla_j(0), \xi_i \rangle| + \sum_{i=N+1, \gamma_i \in \mathcal{I}_{j,+}^{G,(0)}}^{N_{\text{new}}} |\langle \nabla_j(0), \gamma_i \rangle| \right) \quad (ii) \\
& \stackrel{E}{=} \frac{1}{|\mathcal{I}_{j,+}^{U,(0)}|} \left(\sum_{i=1, \xi_i \in \mathcal{I}_{j,+}^{U,(0)}}^{\alpha N} |\langle \nabla_j(0), \xi_i \rangle| + \sum_{i=\alpha N+1, \xi_i \in \mathcal{I}_{j,+}^{U,(0)}}^N |\langle \nabla_j(0), \xi_i \rangle| + (k-1) \sum_{i=N+1, \gamma_i \in \mathcal{I}_{j,+}^{G,(0)}}^{N+\alpha N} |\langle \nabla_j(0), \gamma_i \rangle| \right) \quad (iii) \\
& < \frac{1}{|\mathcal{I}_{j,+}^{U,(0)}|} \left(\sum_{i=1, \xi_i \in \mathcal{I}_{j,+}^{U,(0)}}^{\alpha N} |\langle \nabla_j(0), \xi_i \rangle| + \sum_{i=\alpha N+1, \xi_i \in \mathcal{I}_{j,+}^{U,(0)}}^N |\langle \nabla_j(0), \xi_i \rangle| + (k-1) \sum_{i=\alpha N+1, \xi_i \in \mathcal{I}_{j,+}^{U,(0)}}^N (k+1) |\langle \nabla_j(0), \xi_i \rangle| \right) \quad (iv) \\
& = \frac{1}{|\mathcal{I}_{j,+}^{U,(0)}|} \left(\sum_{i=1, \xi_i \in \mathcal{I}_{j,+}^{U,(0)}}^{\alpha N} |\langle \nabla_j(0), \xi_i \rangle| + k \sum_{i=\alpha N+1, \xi_i \in \mathcal{I}_{j,+}^{U,(0)}}^N k |\langle \nabla_j(0), \xi_i \rangle| \right) = \mathbf{NoiseAlign}(\mathcal{I}_{j,+}^{U,(0)}, \mathbf{w}_j^{(0)}),
\end{aligned}$$

where (i) follows from $|\mathcal{I}_{j,+}^{G,(0)}| \stackrel{E}{=} |\mathcal{I}_{j,+}^{U,(0)}|$ due to random initialization, (ii) is because $\mathcal{I}_{j,+}^{G,(0)}, \mathcal{I}_{j,+}^{U,(0)}$ contain the same noises from the original dataset, (iii) follows from $\sum_{i=1}^{kN} X_i \stackrel{E}{=} k \sum_{i=1}^N X_i$ for some random variable X_i , and (iv) is due to the assumption on the generation noise.

Then at a high level, the higher **NoiseAlign** at initialization for upsampling lets it start off with faster noise learning. This gets propagated to later iterations and in expectation,

$$\langle \mathbf{w}_j^{G,(1)}, \boldsymbol{\gamma} \rangle^2 \|\boldsymbol{\gamma}\|^2 < (k+1) \langle \mathbf{w}_j^{U,(1)}, \boldsymbol{\xi} \rangle^2 \|\boldsymbol{\xi}\|^2$$

for the first iteration, where $\mathbf{w}_j^{G,(1)}, \mathbf{w}_j^{U,(1)}$ are the updated weights for the corresponding dataset. Given the higher **NoiseAlign**, this would hold as long as the higher gradient alignment updates the noise more for RHS upsampling. Subsequently, since Lemma C.1 implies that the noise multi-sets remain unchanged since initialization, the theorem statement follows inductively using the same bounding technique as above.

D Generation vs. Upsampling: Variance Perspective and Proof of Theorem 4.3

For generation, we have a fully independent dataset, so given the per-gradient variance bound σ_G^2 , the variance of the mini-batch gradient \hat{g}_G can be computed as:

$$\begin{aligned}
\mathbb{E} [\|\hat{g}_G - \bar{g}\|^2] &= \mathbb{E} \left[\left\| \frac{1}{B} \sum_{i=1}^B \mathbf{g}_i - \bar{g} \right\|^2 \right] = \mathbb{E} \left[\left\| \frac{1}{B} \sum_{i=1}^B \mathbf{g}_i - \frac{1}{B} B \bar{g} \right\|^2 \right] \\
&= \frac{1}{B^2} \mathbb{E} \left[\left\| \sum_{i=1}^B (\mathbf{g}_i - \bar{g}) \right\|^2 \right] \\
&= \frac{1}{B^2} \sum_{i=1}^B \mathbb{E} [\|\mathbf{g}_i - \bar{g}\|^2] \\
&\leq \frac{1}{B^2} B \sigma^2 \\
&= \frac{\sigma^2}{B},
\end{aligned} \tag{10}$$

where we can directly take the summation out of expectation due to independence among the data.

For the upsampled dataset, we instead have two parts:

1. **Fully independent part:** The first αN data points that contain the fast-learnable feature are independent from each other and the rest.
2. **Replicated part:** The rest of the $k(1 - \alpha)N$ data points that contain duplicates. This part introduces the risk that the same data points might be selected into the same batch.

With this motivation, we let $B = B_1 + B_2$, where B_1 denotes the number of data points selected from the fully independent part, and B_2 denotes the number selected from the replicated part.

For theoretical simplicity, we consider a stratified mini-batch gradient, where B_1 and B_2 are fixed numbers in proportion to the sizes of the two parts. We assume that B_1, B_2 are both integers such that they follow the proportion:

$$B_1 = B \frac{\alpha N}{\alpha N + k(1 - \alpha)N} = B \frac{\alpha}{\alpha + k(1 - \alpha)} \tag{11}$$

$$B_2 = B \frac{k(1 - \alpha)N}{\alpha N + k(1 - \alpha)N} = B \frac{k(1 - \alpha)}{\alpha + k(1 - \alpha)} \tag{12}$$

Note that this removes one source of variance since B_1 and B_2 should themselves be random variables in the actual gradient. Hence, the actual variance should be larger than that of the stratified version.

The variance of the stratified mini-batch gradient \hat{g}_U after upsampling can be split as:

$$\mathbb{E} [\|\hat{g}_U - \bar{g}\|^2] = \mathbb{E} \left[\left\| \frac{1}{B} \sum_{i \in B} \mathbf{g}_i - \frac{1}{B} B \bar{g} \right\|^2 \right] = \frac{1}{B^2} \mathbb{E} \left[\left\| \sum_{i \in B_1} (\mathbf{g}_i - \bar{g}) \right\|^2 \right] + \frac{1}{B^2} \mathbb{E} \left[\left\| \sum_{i \in B_2} (\mathbf{g}_i - \bar{g}) \right\|^2 \right] \tag{13}$$

due to independence and unbiasedness. Here with a slight abuse of notation, $i \in B, B_1, B_2$ represents the indices of data in each portion. Similar to Equation 10, we have for the independent part,

$$\frac{1}{B^2} \mathbb{E} \left[\left\| \sum_{i \in B_1} (\mathbf{g}_i - \bar{g}) \right\|^2 \right] \leq \frac{\sigma^2}{B^2} B_1 = \frac{\sigma^2}{B} \frac{\alpha}{\alpha + k(1 - \alpha)}. \tag{14}$$

For the replicated part, since we may select copied data points, we first rewrite the summation as:

$$\sum_{i \in B_2} \mathbf{g}_i = \sum_{i=1}^{(1-\alpha)N} Y_i \mathbf{g}_i,$$

where we index over all the unique data points $i \in B_2$ and introduce the random variable $Y_i \geq 0$ representing the number of copies of each unique point, subject to $\sum_{i=1}^{(1-\alpha)N} Y_i = B_2$.

Clearly, as we are selecting B_2 data points from a total of $k(1-\alpha)N$ points ($(1-\alpha)N$ unique ones each with k copies), Y_i follows a hypergeometric distribution. From classical probability theory, we have:

1. Mean:

$$\mathbb{E}[Y_i] = B_2 \frac{k}{k(1-\alpha)N} = B \frac{k(1-\alpha)}{\alpha + k(1-\alpha)} \frac{k}{k(1-\alpha)N} = B \frac{k}{\alpha N + k(1-\alpha)N}.$$

2. Variance:

$$\begin{aligned} \text{Var}(Y_i) &= \mathbb{E}[Y_i] \frac{k(1-\alpha)N - k}{k(1-\alpha)N} \frac{k(1-\alpha)N - B_2}{k(1-\alpha)N - 1} \\ &= \mathbb{E}[Y_i] \frac{(1-\alpha)N - 1}{(1-\alpha)N} \frac{k(1-\alpha)N - B \frac{k(1-\alpha)}{\alpha + k(1-\alpha)}}{k(1-\alpha)N - 1} \\ &= \mathbb{E}[Y_i] \frac{(1-\alpha)N - 1}{(1-\alpha)N} \frac{k(1-\alpha)(\alpha N + k(1-\alpha)N - B)}{(k(1-\alpha)N - 1)(\alpha + k(1-\alpha))} \\ &= \mathbb{E}[Y_i] \frac{(1-\alpha)N - 1}{N} \frac{k(\alpha N + k(1-\alpha)N - B)}{(k(1-\alpha)N - 1)(\alpha + k(1-\alpha))} \\ &= \mathbb{E}[Y_i] \frac{k(1-\alpha)N - k}{k(1-\alpha)N - 1} \frac{\alpha N + k(1-\alpha)N - B}{\alpha N + k(1-\alpha)N} \\ &\leq \mathbb{E}[Y_i] \frac{\alpha N + k(1-\alpha)N - B}{\alpha N + k(1-\alpha)N} \\ &= B \frac{k}{\alpha N + k(1-\alpha)N} \left(1 - \frac{B}{\alpha N + k(1-\alpha)N} \right). \end{aligned}$$

3. Second Moment:

$$\begin{aligned} \mathbb{E}[Y_i^2] &= \text{Var}(Y_i) + \mathbb{E}[Y_i]^2 \\ &\leq B \frac{k}{\alpha N + k(1-\alpha)N} \left(1 - \frac{B}{\alpha N + k(1-\alpha)N} \right) + \left(B \frac{k}{\alpha N + k(1-\alpha)N} \right)^2 \\ &= B \frac{k}{\alpha N + k(1-\alpha)N} \left(1 - \frac{B}{\alpha N + k(1-\alpha)N} + \frac{Bk}{\alpha N + k(1-\alpha)N} \right) \\ &= B \frac{k}{\alpha N + k(1-\alpha)N} \left(1 + \frac{(k-1)B}{\alpha N + k(1-\alpha)N} \right). \end{aligned} \tag{15}$$

With these quantities, we can now compute:

$$\begin{aligned} \frac{1}{B^2} \mathbb{E} \left[\left\| \sum_{i \in B_2} (\mathbf{g}_i - \bar{\mathbf{g}}) \right\|^2 \right] &= \frac{1}{B^2} \mathbb{E} \left[\left\| \sum_{i=1}^{(1-\alpha)N} Y_i (\mathbf{g}_i - \bar{\mathbf{g}}) \right\|^2 \right] \quad \text{since } \sum_{i=1}^{(1-\alpha)N} Y_i = B_2 \\ &= \frac{1}{B^2} \sum_{i=1}^{(1-\alpha)N} \mathbb{E} \left[Y_i^2 \|\mathbf{g}_i - \bar{\mathbf{g}}\|^2 \right] \\ &\leq \frac{\sigma^2}{B^2} \sum_{i=1}^{(1-\alpha)N} \mathbb{E} [Y_i^2] \\ &= \frac{\sigma^2}{B} \frac{k(1-\alpha)N}{\alpha N + k(1-\alpha)N} \left(1 + \frac{(k-1)B}{\alpha N + k(1-\alpha)N} \right) \quad \text{by Equation 15} \end{aligned} \tag{16}$$

Algorithm 1 Data Extraction and Image Generation for Training

```
1: Input: Original dataset  $D$ , Model  $f(\cdot, W^{(0)})$ , Separation epoch  $t$ , Total epochs  $T$ , Time steps  $t_*$ ,  
   GLIDE model  $G(\mu_\theta, \Sigma_\theta)$   
2: Step 1: Initial Training  
3: Train the model  $f(\cdot, W^{(0)})$  on dataset  $D$  for  $t$  epochs  
4: Step 2: Clustering and Data Selection Based on Loss  
5: for each class  $c \in D$  do  
6:    $\{C_1, C_2\} \leftarrow \text{k-means}(f(x_j; W^{(t)}))$  {Cluster data into  $C_1$  and  $C_2$ }  
7:   Step 3: Image Generation from Selected Data  
8:   Obtain text prompt  $l$  {e.g. For class dog,  $l$  is a photo of dog}  
9:   for each data point  $x^{\text{ref}} \in C_2$  do  
10:    Initialize random noise  $\epsilon \sim \mathcal{N}(0, I)$   
11:    Generate initial noisy image  $x_{t_*} \leftarrow \sqrt{\bar{\alpha}_{t_*}} x^{\text{ref}} + \sqrt{1 - \bar{\alpha}_{t_*}} \epsilon$   
12:    for  $s$  from  $t_*$  to 1 do  
13:       $\mu, \Sigma \leftarrow \mu_\theta(x_s, s, l), \Sigma_\theta(x_s, s, l)$   
14:       $x_{s-1} \leftarrow \text{sample from } \mathcal{N}(\mu, \Sigma)$   
15:    end for  
16:     $x_{\text{generated}} = x_0$   
17:     $\bar{D} = \bar{D} \cup x_{\text{generated}}$  {Add the generated image to the dataset}  
18:  end for  
19: end for  
20: Step 4: Retraining the Model  
21: Train the model  $f(\cdot, W)$  on updated dataset  $\bar{D}$  for  $T$  epochs  
22: Output: Final model  $f(\cdot, W(T))$ 
```

We plug in Equations 14, 16 into Equation 13 to obtain:

$$\begin{aligned} \mathbb{E} [\|\hat{g}_U - \bar{g}\|^2] &\leq \frac{\sigma^2}{B} \frac{\alpha}{\alpha + k(1 - \alpha)} + \frac{\sigma^2}{B} \frac{k(1 - \alpha)}{\alpha + k(1 - \alpha)} \left(1 + \frac{(k - 1)B}{\alpha N + k(1 - \alpha)N} \right) \\ &= \frac{\sigma^2}{B} \left(1 + \frac{k(k - 1)(1 - \alpha) B}{(\alpha + k(1 - \alpha))^2 N} \right) = I \end{aligned}$$

In the theorem statement, we use $\sigma_U^2(k)$ and $\sigma_G^2(k)$ to differentiate the two and emphasize the dependence on the augmenting factor k .

E Pseudocode

Algorithm 1 illustrates our method.

F Additional Experiments

F.1 Additional experimental settings

Datasets. The CIFAR10 dataset consists of 60,000 32×32 color images in 10 classes, with 6000 images per class. The CIFAR100 dataset is just like the CIFAR10, except it has 100 classes containing 600 images each. For both of these datasets, the training set has 50,000 images (5,000 per class for CIFAR10 and 500 per class for CIFAR100) with the test set having 10,000 images. Tiny-ImageNet comprises 100,000 images distributed across 200 classes of ImageNet [12], with each class containing 500 images. These images have been resized to 64×64 dimensions and are in color. The dataset consists of 500 training images, 50 validation images, and 50 test images per class.

Training on different datasets. From the setting in [2], we trained Pre-Activation ResNet18 on all datasets for 200 epochs with a batch size of 128. We used SGD with the momentum parameter 0.9 and set weight decay to 0.0005. We also fixed $\rho = 0.1$ for SAM in all experiments unless explicitly stated. We used a linear learning rate schedule starting at 0.1. The learning rate is decayed by a factor

Table 1: Details of the upsampling factor k for different methods and datasets.

Method	Dataset	k	Denoising steps
USEFUL	CIFAR10	2	
	CIFAR100	2	
	Tiny-ImageNet	2	
Ours	CIFAR10	5	40, 50, 70, 80
	CIFAR100	5	40, 50, 70, 80
	Tiny-ImageNet	4	50, 70, 80

Table 2: Training ResNet18 on CIFAR10 with different upsampling factor (k).

K	CIFAR10 (USEFUL)	CIFAR10 (OURS)	CIFAR100 (OURS)	TINY-IMAGENET (OURS)
2	4.79	4.57	21.13	32.90
3	5.01	4.52	21.27	30.88
4	5.04	4.45	20.26	30.64
5	4.98	4.42	20.00	31.28

of 10 after 50% and 75% epochs, i.e., we set the learning rate to 0.01 after 100 epochs and to 0.001 after 150 epochs.

Training with different architectures. We used the same training procedures for Pre-Activation ResNet18, VGG19, and DenseNet121. We directly used the official Pytorch [33] implementation for VGG19 and DenseNet121. For ViT [43], we adopted a Pytorch implementation at <https://github.com/lucidrains/vit-pytorch>. In particular, the hidden size, the depth, the number of attention heads, and the MLP size are set to 768, 8, 8, and 2304, respectively. We adjusted the patch size to 4 to fit the resolution of CIFAR10 and set both the initial learning rate and ρ to 0.01.

Hyperparameters. For USEFUL [30], we adopt their default hyper-parameters for separating epochs and set the upsampling factor k to 2 as it yields the best performance. For our method, the upsampling factor k is set to 5 for CIFAR10 and CIFAR100 while that of TinyImageNet is set to 4. Table 1 summarizes the upsampling factor along with the denoising steps at which the synthetic images are used to augment the base training set.

Generating synthetic data with diffusion model. We use an open-source text-to-image diffusion model, GLIDE [31] as our baseline for image generation. We directly used the official Pytorch implementation at <https://github.com/openai/glide-text2im>. While generating, we set the time steps as 100 and the guidance scale as 3.0. For a k -way classification, we input the class names $C = \{c_1, \dots, c_k\}$ with prompt $l = \text{'a photo of'}\{c_i\}'$.

Computational resources. We used 1 NVIDIA RTX 3090 GPU for model training and 4 NVIDIA RTX A5000 GPUs for generating.

F.2 Additional experimental results

Effect of the upsampling factors. Table 2 illustrates the performance of our method and USEFUL when varying the upsampling factors. As discussed in Section 3.2, USEFUL achieves the best performance at $k = 2$ due to overfitting noise at larger k . On the other hand, using synthetic images, our method benefits from larger values of k , yielding the best performance at $k = 5$ for the CIFAR datasets and $k = 4$ for the Tiny-ImageNet dataset. This empirical result reinforces our theoretical findings in Section 4.2.

Effect of the number of denoising steps. Table 3 illustrates the impact of the number of denoising steps on both the FID score and the downstream performance of our method. When initializing the denoising process with real images, increasing the number of steps leads to a higher FID score. Unlike prior works in synthetic data augmentation, we observe that minimizing the FID score between real and synthetic images does not necessarily correlate with improved performance. Specifically, using fewer steps generates images that are overly similar to real images, potentially amplifying the

Table 3: FID and test classification error of ResNet18 on CIFAR10 when augmenting with synthetic images from different denoising steps. The upsampling factor k is set to 2 here.

STEPS	FID	ERM	SAM
0(ORIGINAL IMAGES)		5.07	4.01
10	5.36	4.94	4.03
20	6.86	4.85	3.92
30	7.48	4.83	3.79
40	8.52	4.73	3.92
50	10.67	4.56	3.69
60	13.25	4.68	3.72
70	17.46	4.91	3.84
80	24.27	4.83	3.98
90	34.69	4.87	3.86
100	47.35	4.99	4.28

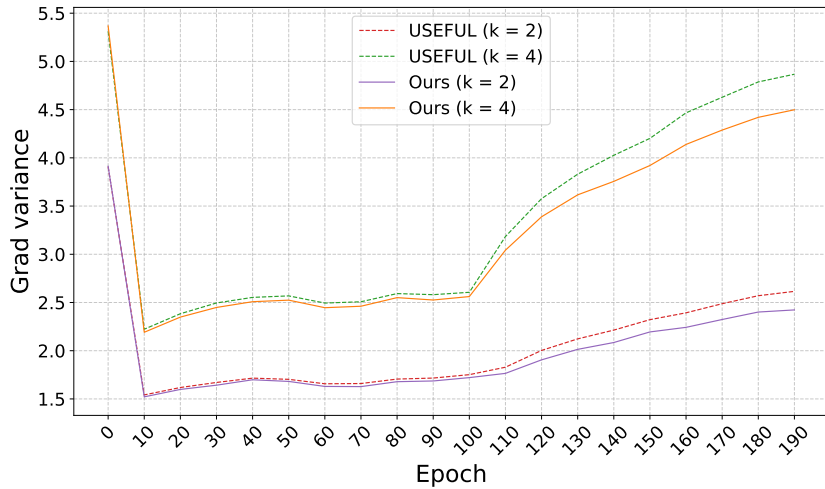


Figure 5: Variance of mini-batch gradients of ResNet18 with SGD on the augmented CIFAR10 dataset found by USEFUL and Ours when varying the upsampling factor k .

inherent noise present in the original data. Conversely, too many denoising steps introduce excessive noise, which also degrades performance. Empirically, we find that using 50 denoising steps strikes the best balance, yielding optimal results for both SGD and SAM optimizers.

Generation time. Using 4 GPUs, the generation time for the entire CIFAR-10, CIFAR-100, and Tiny ImageNet datasets is approximately 12, 12, and 26 hours, respectively. In contrast, our method requires generating only about 30%, 40%, and 60% of the total dataset size, reducing the generation time to just 3.6, 4.8, and 15.6 hours, respectively. This represents a substantial improvement in efficiency compared to prior approaches to synthetic data generation, which typically require producing 10–30 times more samples than the original dataset size.

Variance of mini-batch gradients. Figure 5 presents the mini-batch gradient variance during training of ResNet18 using SGD on the augmented CIFAR-10 datasets selected by USEFUL and our proposed method. Across all upsampling factors k , our method consistently yields lower gradient variance throughout the entire training process. This indicates that our synthetic data provides a more stable and consistent learning signal, which can contribute to more effective optimization. Notably, the variance gap between our method and USEFUL widens significantly after epochs 100 and 150—key points at which the learning rate is decayed. This suggests that our method enables the model to adapt more smoothly to changes in the learning rate, likely due to the benign noise introduced in the faithful synthetic images. Lower gradient variance is often associated with more stable convergence and improved generalization, highlighting the advantage of our approach.